entropy

MDPI

Article

Vanishing Opinions in Latané Model of Opinion Formation

Maciej Dworak and Krzysztof Malarz *

Faculty of Physics and Applied Computer Science, AGH University of Science and Technology, al. Mickiewicza 30, 30-059 Kraków, Poland
* Correspondence: malarz@agh.edu.pl

Abstract: In this paper, the results of computer simulations based on the Nowak–Szamrej–Latané model with multiple (from two to five) opinions available in the system are presented. We introduce the noise discrimination level (which says how small the clusters of agents could be considered negligible) as a quite useful quantity that allows qualitative characterization of the system. We show that depending on the introduced noise discrimination level, the range of actors' interactions (controlled indirectly by an exponent in the distance scaling function, the larger the exponent, the more influential the nearest neighbors are) and the information noise level (modeled as social temperature, which increases results in the increase in randomness in taking the opinion by the agents), the ultimate number of the opinions (measured as the number of clusters of actors sharing the same opinion in clusters greater than the noise discrimination level) may be smaller than the number of opinions available in the system. These are observed in small and large information noise limits but result in either unanimity, or polarization, or randomization of opinions.

Keywords: sociophysics; social impact; opinion dynamics; clusterization and polarization; information noise

check for updates

Citation: Dworak, M.; Malarz, K. Vanishing Opinions in Latané Model of Opinion Formation. *Entropy* **2022**, *25*, 58. https://doi.org/10.3390/e25010058

Academic Editor: Luca Faes

Received: 8 November 2022
Revised: 11 December 2022
Accepted: 26 December 2022
Published: 28 December 2022

Copyright: © 2022 by the authors. Licensee MDPI, Basel, Switzerland. This article is an open access article distributed under the terms and conditions of the Creative Commons Attribution (CC BY) license (https://creativecommons.org/licenses/by/4.0/).

1. Introduction

The formation and dynamics of opinions [1–11] and its spread and propagation [12,13] seem to be a vivid section of sociophysics [14–20]. Existing models [21,22] may be grouped into two families: with discrete or continuous opinions. The latter are represented by Hegselmann–Krause model [23–25], Deffuant et al. model [26–30] (in a one-dimensional opinion space), the Zaller–Deffuant model [31–34] (in a two-dimensional opinion space), compromise model [35–37] or others [38,39]. In the family of discrete models, a particular role is played by toy models dealing with binary opinions and simplified rules of opinion formation, with majority [40,41], voter [42–44], Sznajd [45–49], Galam [50,51] models, among others.

For example, in the voter model [42], the opinions of any given actor on some issue change at random times under the influence of the opinions of his/her neighbors. An actor's opinion at any given time can take one of two values. At random times, a random individual is selected, and that actor's opinion is changed according to a stochastic rule. Specifically, for one of the chosen actor's neighbors, one is chosen according to a given set of probabilities, and that individual's opinion is transferred to the chosen actor.

In the majority model [40], at each time step, a group of r actors is selected, where r can be constant or changed in each successive step. All randomly selected actors adopt the opinion that dominates the group. If the size r of a group of neighbors is even, in case of a tie, either the group adopts an arbitrarily determined biased opinion or maintains the *status quo*.

In the original one-dimensional version of the Sznajd model [45] agent in position i adopts the opinion of the actor sitting in position $i+2$ and the actor in position $i+1$ adopts the opinion of the actor sitting in position $i-1$. These rules ultimately lead the system to

one of three (stable and fixed) attracting points: either two states of *unanimity* or one state of alternately opposite opinions ('antiferromagnetic' state).

These models may be particularly useful for modeling the thinking dichotomy, that is, binary thinking that involves only two extreme attitudes (Typical answers—measuring opinions—for dichotomy-like questionnaires are: 'No' and 'Yes'). Such a situation occurs for voters in countries with two-parties systems (like in the USA), or for actors answering fundamental or simple questions. For example, people usually well know if they like chicken livers with onion (or not), people usually well know if they believe that our Earth is flat (or not), people usually well know if they are pro or contra abortion, etc.

Somewhere on the border between two (discrete/continuous) families of models, discrete opinion models allow multiple opinions to appear [52–63]. These models still allow us to observe geometrical *clusterization* of opinions, but also their *polarization*, which is naturally forced (assumed) in the case of models with binary opinions. Such models are particularly attractive for modeling indifferents as an interface between pro and contra, modeling responses to Likert-scale questionnaires (Typical answers—measuring opinions—for Likert-like questionnaires are: 'Strongly disagree,' 'Disagree,' 'Neither agree nor disagree,' 'Agree,' and 'Strongly agree'), or modeling voter decisions in multiparty systems.

Here, we use a discrete multi-choice opinion model based on computerized version [64] of opinion formation based on Latané theory of social impact [65–67] (see References [55,56,68–70] for examples of model applications and Reference [71] for a comprehensive review).

In Reference [55] Nowak–Szamrej–Latané model [64] was modified to allow multiple (more than two) opinions. It was shown that in the presence of information noise (modeled as social temperature T), the signatures of order/disorder phase transition were observed: in the average fraction of actors sharing the i-th opinion; its variation; the average number of clusters of actors with the same opinion and the average size of the largest cluster of actors who share the same opinion. The social temperature T played a role as a standard Boltzmann distribution parameter that contains the social impact as the equivalent of energy. The order and disordered phases were observed for low ($T < T_C$) and high ($T > T_C$), respectively. For a homogeneous society (with identical actors' supportiveness and persuasiveness), the critical social temperature T_C decreased with an increasing number of available opinions K.

The authors of Reference [56] showed that opinion formation and spread were influenced by both: (i) flow of information between actors (effective range of interactions between actors) and (ii) randomness in adopting opinions (noise level). Noise not only leads to opinion disorder but also promotes consensus under certain conditions. In the disordered phase and when the exchange of information is spatially effectively limited, various faces of disorder were observed, including system states, where the signatures of self-organized criticality manifested themselves as a scale-free probability distribution function for sizes of clusters of actors sharing the same opinion. Then increasing the noise level leads the system to a disordered random state. The critical noise level T_C above which the histograms of the sizes of the opinion groups lost their scale-free character increases with an increase in the ease of information flow.

In this paper, we continue the studies presented in References [55,56]. Namely, with computer simulation based on Nowak–Szamrej–Latané model [64] we check: (i) how influential are the nearest neighbors with respect to the entire population; (ii) the opinion clusterization (including the distribution of these cluster numbers and their sizes); (iii) and distribution of surviving opinions.

The rest of the paper is organized as follows. In Section 2, a detailed description of the model is presented. Section 3 contains the results of simulations. The results obtained are discussed in Section 4 and summarized in Section 5. The list of references and three appendixes—presenting detailed results on: examples of final spatial opinion distribution (Appendix A); average number of clusters (Appendix B); the number of surviving opinions (Appendix C)—close the manuscript.

2. Model

The model is based on previous attempts [55,56,70,72,73] to describe the dynamics of opinion in the context of the theory of social impact [65–67] in its computerized version [64]. The system contains N actors labeled with $i = 0, \cdots, N-1$. Every actor i at time t has an opinion $\xi_i(t) \in \Xi$. The set Ξ of available opinions consists of K different opinions $\{\Xi_1, \cdots, \Xi_K\}$. The social impact $\mathcal{I}_{i,k}(t)$ exerted in time t on an actor i by all actors who share opinions Ξ_k is calculated as

$$\mathcal{I}_{i,k}(t) = \sum_{j=0}^{N-1} \frac{4s_j}{g(d_{i,j})} \cdot \delta(\Xi_k, \xi_j(t)) \cdot \delta(\xi_j(t), \xi_i(t)) \tag{1}$$

or

$$\mathcal{I}_{i,k}(t) = \sum_{j=0}^{N-1} \frac{4p_j}{g(d_{i,j})} \cdot \delta(\Xi_k, \xi_j(t)) \cdot [1 - \delta(\xi_j(t), \xi_i(t))], \tag{2}$$

where Kronecker delta $\delta(x, y) = 0$ when $x \neq y$ and $\delta(x, y) = 1$ when $x = y$. The term $\delta(\Xi_k, \xi_j(t))$ in Equations (1) and (2) indicates that the impact $\mathcal{I}_{i,k}(t)$ on the i-th agent in time t is exerted only by agents j who at time t believe in the opinion Ξ_k ($\xi_j(t) = \Xi_k$). The term $\delta(\xi_j(t), \xi_i(t))$ in Equation (1) vanishes when $\xi_i(t) \neq \xi_j(t)$, i.e., it produces a non-zero contribution of the impact $\mathcal{I}_{i,k}(t)$ on agent i only when agent j shares the opinion of agent i. Thus, therm s_j is considered to be the *supportiveness* of the j-th actor. On the contrary, the term $[1 - \delta(\xi_j(t), \xi_i(t))]$ resets the impact when agents i and j share the same opinion. It means that the components of the sum (2) can be non-zero only when interacting in time t agents have different opinions $\xi_i(t) \neq \xi_j(t)$ and, thus, p_j play a role of *persuasiveness* of the j-th agent. The supportiveness s_i and persuasiveness p_i are taken randomly from the interval $[0, 1]$. $d_{i,j}$ stands for the Euclidean distance between agents i and j. The distance scaling function $g(\cdot)$ should be a non-decreasing function that ensures a decreasing influence from more and more distant actors. Here, we assume that

$$g(x) = 1 + x^{\alpha}, \tag{3}$$

where the exponent α is a model control parameter.

After calculating impacts (1), (2) for each actor i and every opinion Ξ_k available in the system, the temporal evolution of i-th actor opinion ξ_i can be predicted based on either deterministic (in absence of information noise) or non-deterministic (in presence of information noise) way.

In the deterministic version (without information noise), the actor i in the next time step $(t+1)$ takes the opinion Ξ_k that the believers exerted the largest impact on him/her:

$$\begin{aligned} \xi_i(t+1) = \Xi_k \iff \\ \mathcal{I}_{i,k}(t) = \max(\mathcal{I}_{i,1}(t), \mathcal{I}_{i,2}(t), \ldots, \mathcal{I}_{i,K}(t)). \end{aligned} \tag{4}$$

When information noise is present in the system, the social impact $\mathcal{I}_{i,k}(t)$ (1), (2) determines the probability $P_{i,k}(t)$ of accepting opinion Ξ_k in the next time step $(t+1)$ by i-th actor. To that end, we introduce a (temperature-like) information noise parameter T [74] and a Boltzmann-like factor

$$p_{i,k}(t) = \exp\left(\frac{\mathcal{I}_{i,k}(t)}{T}\right), \tag{5a}$$

which allow us to define the above-mentioned probability

$$P_{i,k}(t) = \frac{p_{i,k}(t)}{\sum_{j=1}^{K} p_{i,j}(t)}. \tag{5b}$$

Then, i-th actor accepts in the next time step $(t+1)$ opinion Ξ_k

$$\xi_i(t+1) = \Xi_k, \text{ with probability } P_{i,k}(t). \tag{6}$$

We assume that the actors occupy nodes of the square grid

$$\mathcal{G} = \{(x,y) : 0 \leq x,y < L, \quad x,y \in \mathbb{Z}\}$$

and agent's label $i = Lx + y$. The open boundary conditions are assumed. Initially (at $t = 0$), the agents take random opinions. The examples of the initial system states are presented in Figure 1 for $K = 2$ (Figure 1a) and for $K = 4$ (Figure 1b). Various opinions are marked by various colors. The algorithm of performed simulations is presented in Algorithm 1 [73]. The source code of the program (written in C) is available in Reference [75].

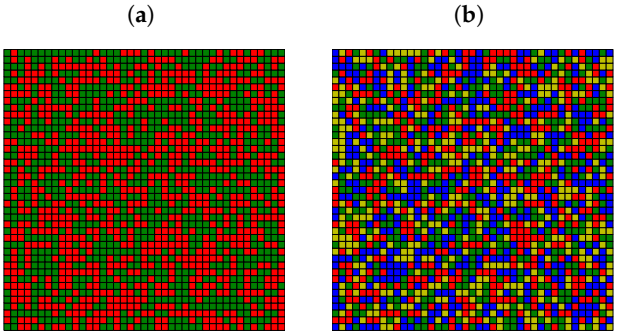

Figure 1. Example of random initial state of the system for (**a**) $K = 2$ and (**b**) $K = 4$. Various colors correspond to various opinions.

3. Results

In this Section, we describe the results of computer simulations carried for square lattice with $L^2 = 41^2$ actors. If not stated otherwise, the results are gathered after $t = 1000$ time steps and averaged over $R = 100$ independent system realizations (for various random initial spatial distribution of opinions $\xi_i(t = 0)$, supportiveness s_i and persuasiveness p_i values).

3.1. How Influential Are the Nearest-Neighbours in Respect to the Entire Population?

To better understand the role played by the α parameter, we check the ratio

$$\beta(n) = \frac{(L-2r)^{-2} \cdot \sum_{x=r}^{(L-r)} \sum_{y=r}^{(L-r)} \sum_{k=1}^{K} \mathcal{I}_{i,k}^{n}(t \to \infty)}{L^{-2} \cdot \sum_{i=1}^{L^2} \sum_{k=1}^{K} \mathcal{I}_{i,k}(t \to \infty)}, \tag{7}$$

which describes the opinion-independent relative influence of n geometrically nearest neighbors with respect to the total impact coming from all actors. Examples of shapes of these nearest neighborhoods containing $n = 1, 9, 25, 49$ actors are sketched in Figure 2. The measured influence ratio $\beta(n)$ is averaged over $(L-2r)^2$ actors with $r = 0$ for $n = 1$, $r = 1$ for $n = 9$, $r = 2$ for $n = 25$, $r = 3$ for $n = 49$, etc., reflecting the possibility of placing the yellow square from Figure 2 in the square grid $\mathcal{G}$ without protruding beyond the boundaries of the system. The term $\mathcal{I}_{i,k}^{n}$ stands for social impact calculated according to Equations (1), (2) but with an upper summation index replaced by $(n-1)$ instead of $(N-1)$. The impacts $\mathcal{I}_{i,k}^{n}$ and $\mathcal{I}_{i,k}$ are measured at the long-term simulation limit $(t \to \infty)$. The results of the simulations of $\beta(n)$ are presented in Table 1.

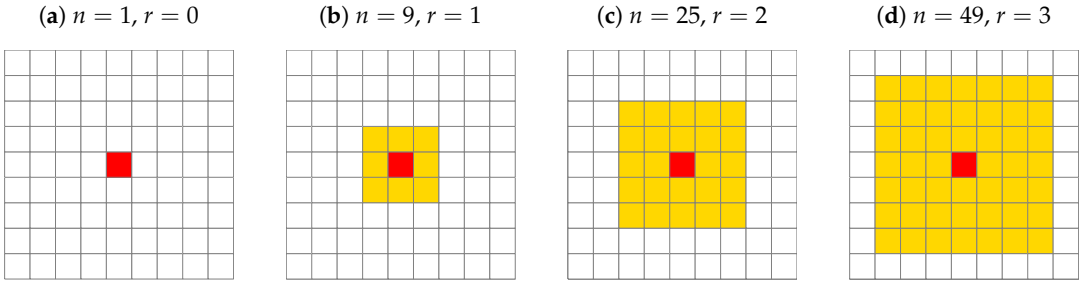

Figure 2. The sketches of shapes of the neighborhoods closest to the sites (**a**) $n = 1$, (**b**) $n = 9$, (**c**) $n = 25$, (**d**) $n = 49$ sites. The values of the r parameters indicated in the figures in the headline influence summation limits in the nominator of Equation (7).

Table 1. Average ratio $\beta(n)$ [defined in Equation (7)] of the influence of the neighborhood with n sites (presented in Figure 2) to the total influence of the entire network with L^2 sites for various values of K and α.

α	2	3	4	6
n		$K = 2$		
1	0.05987(13)	0.14973(63)	0.2209(13)	0.2902(16)
9	0.25269(45)	0.58795(79)	0.80513(74)	0.95820(21)
25	0.39642(56)	0.76437(75)	0.92761(38)	0.993687(41)
49	0.49898(57)	0.84573(64)	0.96450(21)	0.998328(12)
81	0.57600(53)	0.89073(54)	0.97971(13)	0.9994007(45)
121	0.63641(46)	0.91866(44)	0.987262(83)	0.9997408(20)
169	0.68530(41)	0.93739(36)	0.991477(58)	0.9998727(10)
225	0.72578(35)	0.95064(29)	0.994033(42)	0.99993158(54)
289	0.75989(31)	0.96039(24)	0.995680(31)	0.99996061(31)
361	0.78903(28)	0.96778(20)	0.996790(23)	0.99997609(18)
n		$K = 3$		
1	0.05990(17)	0.15080(92)	0.2232(16)	0.2937(22)
9	0.25275(62)	0.5873(15)	0.8041(10)	0.95793(26)
25	0.39649(85)	0.7635(13)	0.92698(53)	0.993625(52)
49	0.49906(96)	0.8449(11)	0.96414(29)	0.998311(15)
81	0.5761(10)	0.89006(90)	0.97950(18)	0.9993947(53)
121	0.6365(10)	0.91812(72)	0.98712(12)	0.9997382(22)
169	0.6854(10)	0.93694(59)	0.991385(81)	0.9998715(10)
225	0.72586(96)	0.95027(48)	0.993969(57)	0.99993091(62)
289	0.75996(93)	0.96008(39)	0.995633(41)	0.99996022(35)
361	0.78909(88)	0.96753(32)	0.996755(31)	0.99997585(21)
n		$K = 4$		
1	0.05990(16)	0.15095(98)	0.2247(20)	0.2962(27)
9	0.25275(50)	0.5871(15)	0.80338(98)	0.95757(28)
25	0.39649(65)	0.7633(14)	0.92657(51)	0.993549(51)
49	0.49906(70)	0.8448(11)	0.96393(29)	0.998291(15)
81	0.57609(70)	0.88999(90)	0.97938(18)	0.9993876(54)
121	0.63649(69)	0.91807(74)	0.98705(12)	0.9997353(22)
169	0.68538(66)	0.93690(60)	0.991331(79)	0.9998701(12)
225	0.72586(63)	0.95024(49)	0.993931(56)	0.99993012(63)
289	0.75997(59)	0.96006(41)	0.995605(40)	0.99995976(36)
361	0.78911(56)	0.96751(34)	0.996735(30)	0.99997557(21)
n		$K = 5$		
1	0.05988(15)	0.1511(10)	0.2248(21)	0.2976(26)
9	0.25267(48)	0.5867(15)	0.8029(11)	0.95741(29)
25	0.39638(58)	0.7629(13)	0.92634(61)	0.993525(55)
49	0.49893(59)	0.8445(11)	0.96380(34)	0.998284(15)
81	0.57595(57)	0.88970(90)	0.97930(21)	0.9993847(57)
121	0.63634(55)	0.91784(73)	0.98700(14)	0.9997340(25)
169	0.68523(53)	0.93673(60)	0.991302(92)	0.9998694(12)
225	0.72571(51)	0.95010(49)	0.993909(65)	0.99992979(66)
289	0.75982(49)	0.95995(40)	0.995590(46)	0.99995958(37)
361	0.78896(49)	0.96742(33)	0.996723(35)	0.99997546(24)

Within the estimated uncertainties, the ratio $\beta(n)$ does not depend on the number K of opinions available in the system and appears to be a purely geometric characteristic of the model. Of course, we expected an observed increase in $\beta(n)$ with an increase in n independently on K and α. Much more interesting is the observed monotonic increase in $\beta(n)$ with the increase in the distance scaling function exponent α. For $\alpha = 2$, roughly 25% of the impact comes from $n = 9$ nearest-neighbors. This ratio increases to $\beta(9) \approx 59\%$ for $\alpha = 3$, $\beta(9) \approx 80\%$ for $\alpha = 4$ and $\beta(9) \approx 96\%$ for $\alpha = 6$. For $n = 25$, roughly $\beta(25) \approx 39\%$, 76%, 92%, and 99% of the social impact exerted comes from only those twenty-five neighbors for $\alpha = 2$, 3, 4, and 6, respectively. In other words, the α parameter says how influential the nearest neighbors are with respect to the entire population: the larger α, the more influential the nearest neighbors are.

3.2. The Final Opinions Distributions

The initial random opinions presented in Figure 1 evolve according to Equation (4) (in the absence of information noise $T = 0$) or Equation (6) (for $T > 0$). This temporal evolution subsequently changes the spatial opinion distribution. In Figure 3, examples of the two most probable final opinion spatial distributions for various noise levels T after 10^3 time steps are presented. The exponent in the distance scaling function is assumed to be $\alpha = 3$. The system contains $L^2 = 41^2$ actors and $K = 4$ possible opinions.

For a deterministic version of the algorithm ($T = 0$, see Figure 3a,b), all K opinions initially present in the systems survive; however, the clustering of actors who share the same opinions is observed. A slight increase in temperature ($T = 1$) 'melts' the 'frozen' state leading either to consensus (the same opinion shared by all actors, see Figure 3c) or polarization (two, well separated, clusters of opinions, see Figure 3d). As a cluster of opinions—or more precisely, actors—we consider a group of actors who share the same opinions and are connected by the nearest-neighbor interaction (sitting in the von Neumann neighborhood, as for random site percolation problem). The number of actors who share the same opinion and belong to the same cluster defines the cluster size $\mathcal{S}$. The increase in noise level to $T = 2$ allows a small number of actors to appear with other available but short-lived opinions (appearing at time t and immediately disappearing at $t + 1$) (see Figure 3e,f) as the temperature increases T—according to Equation (5)—favorites the appearance of less probable opinions (exerting less impact). The above-mentioned increase in probability (5) with T leads to an increase in the number of single actors or even pairs of actors with minority opinions destroying locally either consensus (see Figure 3g) or system polarization (see Figure 3h). The further increase in T also allows for the appearance of larger (but still relatively small) clusters of opinions (Figure 3i,j). Finally, for a high noise level, all opinions become equiprobable as

$$\lim_{T\to\infty} P_{i,k}(t) = 1/K$$

in every time step t for every actor i and for every opinion Ξ_k. The latter leads to the system blinking with all K available 'colors of opinion at every time step t and at every site i—the snapshot of the system does not differ much from the one presented in Figure 1b.

Examples of the spatial distributions of the final opinion for $\alpha = 3$ and $K = 2$, 3, and 5 (Figures A1–A3) and for $\alpha = 4$ and $K = 2$, 3, 4, and 5 (Figures A4–A7) are collected in Appendix A.

3.3. Opinion Clustering

As the most commonly observed phenomenon in the system is opinion clustering, we check the distribution of these cluster numbers and sizes. To this end, we utilize the Hoshen–Kopelman algorithm [76] (pp. 59–60), [77–79]. With Hoshen–Kopelman algorithm, one can label every site in such a way that sites (actors sharing the same opinions) in various clusters are labeled with various labels, and sites belonging to a given cluster are labeled with the same label.

Let us look again at Figure 3c,d obtained for $\alpha = 3$, $K = 4$ and $T = 1$. In Figure 3c, consensus takes place, and we observe a single cluster (the number of clusters $\mathcal{C} = 1$), and all actors belong to this cluster (the size of the cluster $\mathcal{S} = L^2$). In Figure 3d, the system polarization is observed, thus, the number of observed clusters is two ($\mathcal{C} = 2$), but most of the actors are in a 'red' cluster ($\mathcal{S}_1 \approx 0.92L^2$) while actors with minority opinion (marked with 'green') are occupying the upper left corner of the system ($\mathcal{S}_2 \approx 0.08L^2$).

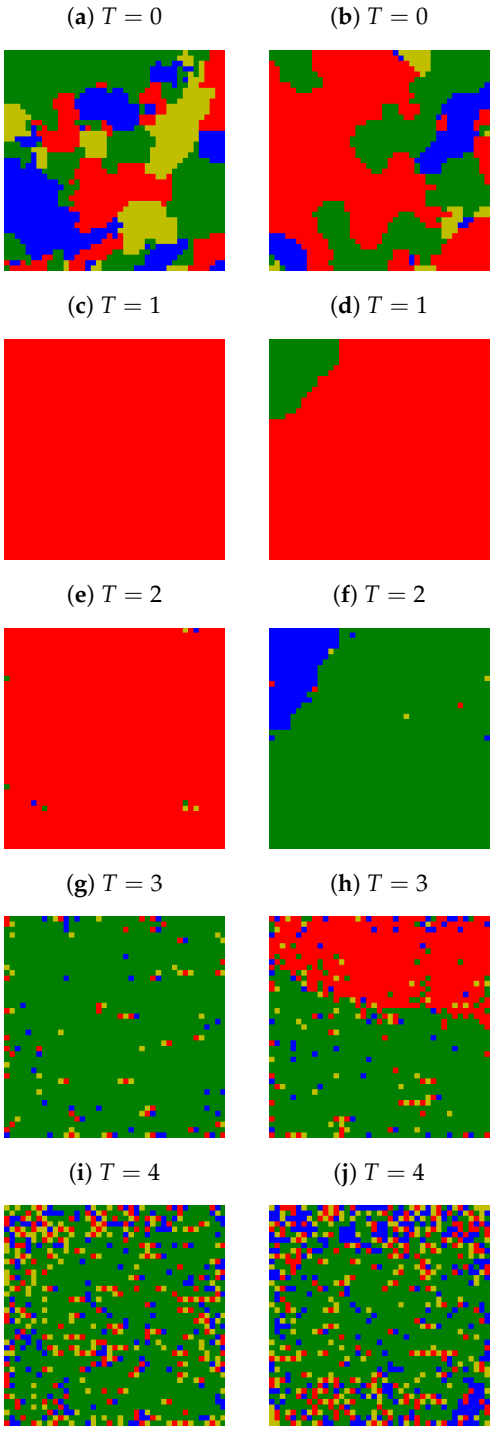

Figure 3. Examples of two most probable spatial distributions of the final opinion after 10^3 time steps. $L = 41$, $\alpha = 3$, $K = 4$ and various levels of noise T.

As for larger noise levels, single sites with minority opinions appear from time to time (cf., for example, Figure 3e,h), but the main picture behind remains the same (i.e.,

in principle, we still deal either with consensuses or system polarization), it would be useful to introduce the noise discrimination level θ. For example, setting $\theta = 5$ and neglecting appearance clusters with sizes $\mathcal{S}$ smaller than θ is sufficient to keep the picture of the number $\mathcal{C}$ of clusters as for those presented in Figure 3c,d also for systems presented in Figure 3e,h.

The results presented below are based on assuming various levels of discrimination θ in the spirit described above. In other words, the θ parameter arbitrarily says how small the clusters of agents sharing the same opinion could be considered negligible.

3.3.1. Average Number of Opinion Clusters

In Figure 4, the average number $\mathcal{C}$ of opinion groups is presented for $\alpha = 3$ and $K = 4$. Statistics are based on $R = 100$ replications of the system with $L^2 = 41^2$ actors measured after $t = 10^3$ time steps of evolution. We assume the discrimination threshold $\theta = 25$.

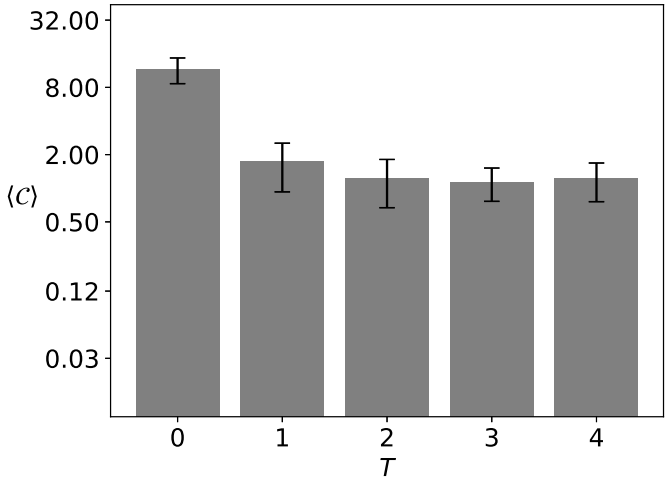

Figure 4. Average number $\langle \mathcal{C} \rangle$ of opinion clusters after $t = 10^3$ time steps for the exponent of the distance scaling function $\alpha = 3$, the number $K = 4$ of opinions available in the system, and the noise discrimination threshold $\theta = 25$. The system contains $L^2 = 41^2$ actors. The results are averaged over $R = 100$ independent system realizations.

For $T = 1$ roughly half among $R = 100$ simulations end in consensus ($\mathcal{C} = 1$) or system polarization ($\mathcal{C} = 2$) leading to the average number of clusters $\langle \mathcal{C} \rangle \approx 1.73(80)$. The symbol $\langle \cdots \rangle$ stands for the averaging procedure on $R = 100$ independent system realizations (simulations). The increase in the level of noise $T \geq 2$ with the assumed discrimination threshold $\theta = 25$ does not change the average number of clusters $\langle \mathcal{C} \rangle$ to much: $\langle \mathcal{C} \rangle = 1.24(57)$, $1.14(38)$ and $1.22(46)$ for $T = 2$, 3 and 4, respectively.

However, for $T = 0$ this number $\langle \mathcal{C} \rangle \approx 11.6$ (with uncertainty 3.0) is much higher than for $T \neq 0$ (please note the logarithmic scale on the $\langle \mathcal{C} \rangle$ axis). We should stress that the number of clusters $\mathcal{C} = 17$ (Figure 3a) and $\mathcal{C} = 8$ (Figure 3b) is higher than the number of opinions available $K = 4$ in the systems. In other words, several different clusters of the same opinion are counted for the number $\mathcal{C}$. For instance, in Figure 3b, we observe four clusters (of sizes $\mathcal{C}$ larger than $\theta = 25$) of 'green' opinions, two of 'blue' opinions, two of 'red' opinions, and none of 'yellow' opinions.

The average number $\langle \mathcal{C} \rangle$ of clusters for various values of the distance scaling function exponent $\alpha = 2$, 3, 4, and 6, number of available opinions $K = 2$, 3, 4, and 5, information noise level $T = 0$, 1, 2, 3, and 4 and noise discrimination levels $\theta = 12$, 25 and 50 are presented in Figures A8–A10 in Appendix B.

3.3.2. The Sizes of the Largest Clusters

In Reference [56] average largest cluster size $\langle \mathcal{S}_{\max} \rangle$ (normalized to the system size L^2) for $K = 2$ and $K = 3$ and various values of the noise level T and the interaction range

α were presented in Figures 6a and 7a, respectively. Here, we also extend this study to a larger number K of opinions available in the system, namely for $K = 4$ and $K = 5$. The results are presented in Figure 5.

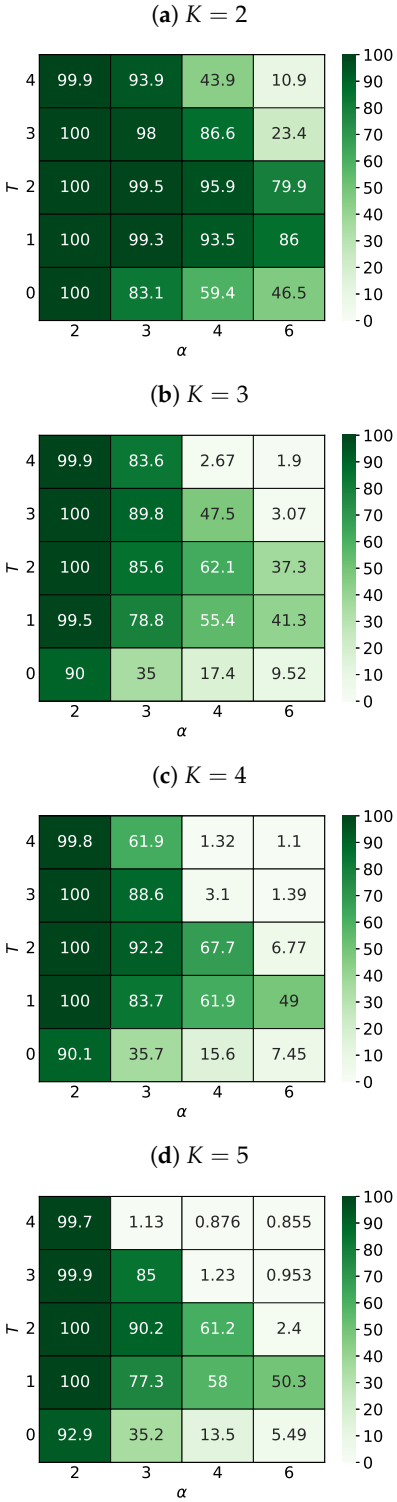

Figure 5. The average ratio (in percents) of the size of the largest cluster $\langle \mathcal{S}_{\max} \rangle$ to the size of the entire system L^2 depending on the parameters α and T. $L = 41$, $t = 10^3$, $R = 100$.

Let us again look at the thermal evolution of $\mathcal{S}_{\max}$ of the system presented in Figure 3. Due to the freezing system for $T = 0$ (as presented in Figure 3a,b), the largest cluster sizes are around $\mathcal{S}_{\max} = 267$ and $\mathcal{S}_{\max} = 794$ (cluster of 'green' opinion in the upper left corner

and cluster of 'red' opinion in the left side of Figures 3a,b, respectively). The increase in noise level to $T = 1$ increases the sizes of the largest cluster to $\mathcal{S}_{\max} = L^2$ and $\mathcal{S}_{\max} = 1540$ for Figures 3c,d, respectively. Then, the subsequent increase in T only reduces the size of the largest cluster.

3.4. Distribution of Surviving Opinions

The methodology of cluster counting allows for the construction of histograms $\langle \mathcal{C}(T) \rangle$ presented in Figures 4 and A8–A10—as mentioned in Section 3.3.1—neglects the colors of the clusters. Thus, the information provided there is insufficient to determine whether all K opinions available in the system persisted until the assumed time $t = 10^3$. Now, we are interested in checking the number $1 \leq \Phi \leq K$ of surviving opinions for various values of the parameters K, α, and T.

As mentioned above, the system presented in Figure 3b for $K = 4$, $\alpha = 3$, $T = 0$ has eight clusters larger than $\theta = 25$, and, thus, the number of clusters $\mathcal{C}$ is eight. As three opinions available in the system are observed, then $\Phi = 3$. In contrast, for $T = 1$ (see Figure 3d), only $\Phi = 2$ opinions ('red' and 'green') survived. There, due to the polarization of the system, the number of clusters $\mathcal{C}$ and the number of surviving opinions Φ are equal.

3.4.1. Histograms of Surviving Opinions

The opinion that survives in the system is the opinion that, at the end of the simulation, it is represented by at least one cluster with size $\mathcal{S}$ not smaller than θ.

In Figure 6, the histogram of the number $\Phi(T)$ of surviving opinions for $\alpha = 3$, $K = 4$ and the level of noise discrimination $\theta = 25$ are presented.

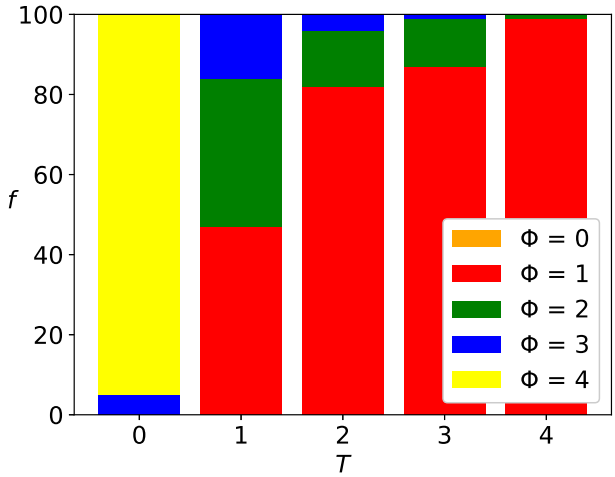

Figure 6. The histogram of frequencies f of the number Φ of surviving opinions for $\alpha = 3$, $K = 4$ and the level of noise discrimination $\theta = 25$.

The results are collected again after $t = 10^3$ time steps and for $R = 100$ system realizations.

For $T = 0$, 95% of these R simulations ended with $\Phi = 4$ [$f(\Phi = 4) = 95\%$, yellow rectangle in the first bar of Figure 6] surviving opinions, and 5% of the simulations ended with $\Phi = 3$ surviving opinions [$f(\Phi = 3) = 5\%$, blue rectangle in the first bar of Figure 6]. Situations with consensus ($\Phi = 1$) or system polarization ($\Phi = 2$) were not observed: $f(\Phi = 1) = f(\Phi = 2) = 0\%$ [absence of green and red rectangles in the first bar of Figure 6]. Finally, the orange color is also absent [$f(\Phi = 0) = 0\%$] in the first bar of Figure 6], which means that the situation of all opinions disappearing was not observed. Of course, the rules of the game do not allow for vanishing all opinions: the case $f(\Phi = 0) > 0$ means that the fraction $f(\Phi = 0)$ of system realizations ended with a lot of very small clusters, each of them smaller than the assumed noise discrimination level θ.

For $T = 1$, 47% of these R simulations ended with $\Phi = 1$ [$f(\Phi = 1) = 47\%$, red rectangle on the second bar of Figure 6] surviving opinions, 37% of the simulations ended

with $\Phi = 2$ surviving opinions [$f(\Phi = 2) = 37\%$, green rectangle in the second bar of Figure 6] and 16% of the simulations ended with $\Phi = 3$ surviving opinions [$f(\Phi = 3) = 16\%$, blue rectangle in the second bar of Figure 6], etc.

For the highest noise level investigated ($T = 4$) we have $f(\Phi = 1) \approx 99\%$ (red rectangle in the fifth bar in Figure 6) and $f(\Phi = 2) \approx 1\%$ (green rectangle in the fifth bar in Figure 6).

Histograms of frequencies $f(\Phi)$ of the numbers Φ of the surviving opinions for various values of K, α, T and three values of noise discrimination level $\theta = 12, 25, 50$ are presented in Figures A11–A13 in Appendix C.

3.4.2. The Most Probable Number of Surviving Opinions

We finalize the presentation of the results with heat maps of the most probable final number of surviving opinions $\Phi^\star$ (see Figure 7). We define the most probable number of surviving opinions $\Phi^\star$ as this value of Φ for which the fraction $f(\Phi)$ is the largest (for fixed values of the noise discrimination level θ, the noise level of information T and the effective range of interaction α).

For example, for $K = 4$, $\alpha = 3$, $\theta = 25$ and

- for $T = 0$ (see the first bar of Figure 6) $\Phi^\star = 4$ as $95\% = f(\Phi = 4) > f(\Phi = 3) = 5\%$,
- for $T = 1, 2, 3$ (see the second, third, and fourth bar of Figure 6) $\Phi^\star = 1$ as $f(\Phi = 1) > f(\Phi = 2) > f(\Phi = 3)$,
- for $T = 4$ (see the fifth bar of Figure 6) $\Phi^\star = 1$ as $99\% = f(\Phi = 1) > f(\Phi = 2) = 1\%$.

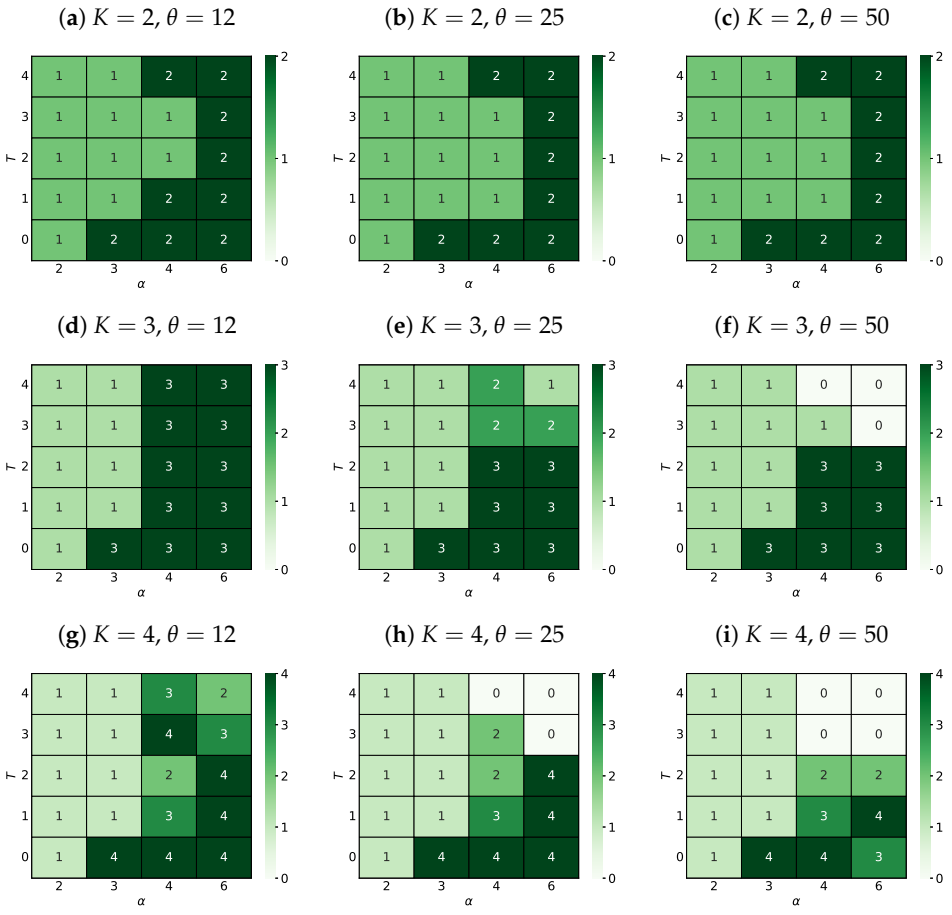

Figure 7. *Cont.*

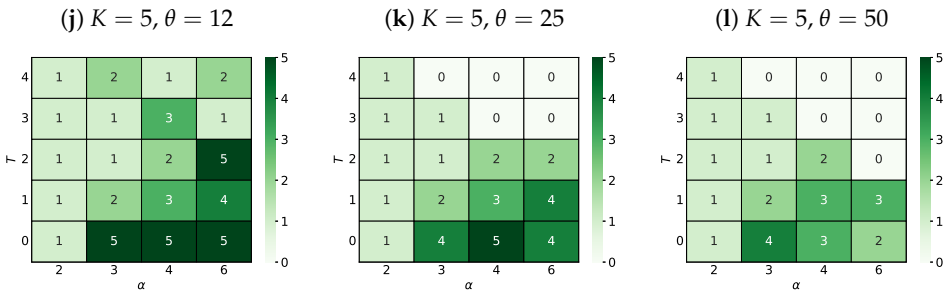

Figure 7. The most probable final number $\Phi^\star$ of surviving opinions for various numbers K of opinions available in the system and noise discrimination thresholds θ depending on the level of information noise T and the range of interaction α.

4. Discussion

4.1. Average Number of Opinion Clusters

For a low value of the noise discrimination level ($\theta = 12$, Figure A8) and $\alpha = 2$ (see Figures A8a–d) for the nondeterministic version of the algorithm ($T > 0$), only one cluster exceeds the threshold size, regardless of the number K of opinions available in the system. Therefore, the system is dominated by a single group of opinions, and consensus takes place.

Reducing the impact of distant actors ($\alpha = 3$, Figure A8e–h) allows additional clusters of size S greater than $\theta = 12$. Their number $\langle \mathcal{C} \rangle$ most often does not exceed two, except for the simulation of a high number of opinions available ($K > 3$) and high social temperature ($T = 4$). For such parameter settings, we can observe, on average more than two clusters, at the same time with a greater standard deviation of this number — the number of clusters, depending on the simulation, ranges from $\langle \mathcal{C} \rangle = 1$ to about $\langle \mathcal{C} \rangle = 5 \div 6$. Independently of the number of K the deterministic case ($T = 0$) produces a relatively high average number $\langle \mathcal{C} \rangle$ of clusters ($\langle \mathcal{C} \rangle = 4$ for $K = 2$ opinions, $\langle \mathcal{C} \rangle = 16$ and for $K > 2$).

An increased exponent ($\alpha = 4$, Figure A8i–l) results in a clear increase in the average number $\langle \mathcal{C} \rangle$ of clusters in the system up to $\langle \mathcal{C} \rangle = 32$ for $T = 0$.

For the largest value considered of $\alpha = 6$ (Figure A8m–p) the most numerous sets of clusters with a size S exceeding $\theta = 12$ are observed. With two opinions in the system (Figure A8m), the temperature $T = 3$ is sufficient for a significant division of agents for $\langle \mathcal{C} \rangle \geq 16$ clusters with a size exceeding the threshold θ. The trend continues for simulations with available $K = 3$ different opinions (Figure A8n). However, for high temperatures and a large number of possible opinions ($K = 4$, $T = 4$ and $K = 5$, $T = 3, 4$), the average number of clusters $\langle \mathcal{C} \rangle$ with size S greater than the threshold θ begins to decline due to too much fragmentation—the system becomes an irregular set of many very small clusters (Figures A6i,j and A7i,j), and none of the opinions can get a noticeable advantage. For $T = 0$, the average number of clusters in the system remains very high and reaches $\langle \mathcal{C} \rangle = 32$.

For increased threshold $\theta = 25$ (Figure A9) noticeable differences appear for $K = 4, 5$ and $\alpha = 3$ and the highest of the social temperatures studied $T = 4$ (Figure A9g,h), where fewer clusters were recorded that met the condition $S > \theta = 25$.

For the simulations with $K = 5$ and $T = 4$, where at least one cluster of an appropriate size has been preserved, it was so rare that the average number of clusters was a fraction ($\langle \mathcal{C} \rangle \approx 0.15$). This value well reflects the division of agents who share the same opinion into small, randomly arranged clusters.

A further increase in the threshold θ (up to 50, Figure A10) results in disappearing clusters of sizes S larger than θ for $\alpha \geq 4$ and $K \geq 4$ (Figure A10k,l,o,p).

4.2. The Sizes of the Largest Clusters

We would like to recall the ambivalent role observed of the information noise level T in shaping the largest cluster size $\mathcal{S}_{\max}$ mentioned in Reference [56] (p. 14): '[...] the average size of the maximum cluster $\mathcal{S}_{\max}$ decreases with α for fixed T values. The appearance

of noise in the system ($T = 1$) slightly organizes the system in relation to the noiseless situation with $T = 0$ (which is particularly visible for $\alpha > 2$ [...]). Indeed, as in earlier studies [80,81], a small level of noise brought more order to the system. Furthermore, the introduction of noise (T) in the adoption of opinions causes an increase in $\mathcal{S}_{\max}$, and then its decrease, which is especially visible for $\alpha > 2$ (this inflection point is nearly $T = 2$).' and later: '[...] noise for certain values of α promotes unanimity. This situation occurs for $\alpha = 3$ (both for $K = 2$ and $K = 3$), when the frozen state system, with increasing noise T, achieves the consensus state for $T = 3$, before disordering for $T = 5$' [56] (p. 18).

This nonmonotonous dependence $\mathcal{S}_{\max}/L^2$ on the noise parameter T is observed for any value of α, but for larger values of α and larger values of the number K of opinions available in the systems, this dependence becomes more and more spectacular. For example, for $K = 5$ (Figure 5d) we see a high peak of $\mathcal{S}_{\max}/L^2 \approx 50\%$ for $T = 1$ and $\alpha = 6$ deeply reduced to 2.4% and 5.5% for a larger ($T = 2$) and lower ($T = 0$) noise level. The similar behavior in $\mathcal{S}_{\max}$ in dependence on T is also observed for $\alpha = 4$ with $\mathcal{S}_{\max}/L^2 \approx 60\%$ for $T = 1, 2$ reduced to 1.2% and 13.3% for a higher ($T = 3$) and lower ($T = 0$) noise level. The further increasing influence of more distance actors (decreasing α) makes the $\mathcal{S}_{\max}$ dependence smoother and smoother, making it almost flat for $\alpha = 2$ with only marginal deviation from $\mathcal{S}_{\max}/L^2 = 100\%$ at the edges of the range of values studied for the parameter T.

The picture presented above is also qualitatively reproduced for $K = 4$ (see Figure 5c).

Independently of the number K of opinions considered available in the system for a fixed value of the noise parameter T, the average size of the largest cluster $\mathcal{S}_{\max}$ decreases with increasing of α, i.e., with limiting the influence of very long-range interactions.

4.3. Histograms of Surviving Opinions

The histograms $f(\Phi; T)$ of the surviving opinions (Section 3.4.1) presented in Figures A11–A13 in Appendix C are almost untouched by the noise discrimination level θ for a highly effective interaction range [$\alpha = 2$, Figures A11a–d, A12a–d and A13a–d] as well as for the lowest possible number of opinions available in the system [$K = 2$, Figures A11a,e,i,m, A12a,e,i,m and A13a,e,i,m]. This is a consequence of the appearance of consensus or system polarization and is consistent with the generally observed final system states presented earlier in Figures 3 and A1–A7.

The most noticeable differences occur in Figures A11g,h,k,l,o,p, A12g,h,k,l,o,p and A13g,h,k,l,o,p, that is, for $\alpha \geq 3$ and $K \geq 4$. For a high noise level ($T = 4$) in this parameter regime, the frequency $f(\Phi = 0)$ dominates the system (absence of sizes S greater than θ) except for the lowest assumed threshold $\theta = 12$, allowing observation up to $\Phi = 3$ surviving opinions, but of small cluster sizes.

4.4. The Most Probable Number of Surviving Opinions

We finalize the discussion of the results obtained with an analysis of the heat maps (Figure 7) of the most probable final number Φ^* (Section 3.4.2, Figure 7) of the remaining opinions for various numbers K of opinions available in the system and various noise discrimination numbers θ. These maps are constructed in the (α, T) plane. With the assumed scanning accuracy of the parameters, α i T parameters, the shape of the obtained maps differs qualitatively from those reported in Figures 6 and 7 in Reference [56], particularly with well-visible juts for higher values of Φ^* for intermediate values of the level of information noise $2 \leq T \leq 3$ and high values of $\alpha \approx 6$ (that is, for a long effective range of interaction between actors).

5. Conclusions

In Reference [55], the model of opinion formation was introduced based on the Latané theory of social impact with many available opinions. In computer simulations based on the Szamrej–Nowak–Latané model, it was shown that increasing the number of opinions decreases the critical noise level separating ordered and disordered phases. The observed

results were followed by further studies [56] in which both the noise level T and the interaction range α were considered. It was shown that the noise level has an ambiguous role: its lower value helps in system ordering (spatial clustering of opinions), while its higher value destroys any spatial correlations among actors and their opinions. This useful role for the small noise level was also reported in References [81–84].

In this paper, we follow the path indicated in the References [55,56] and with a computerized version of the social impact theory (Section 2) we simulate the formation of opinions in an artificial society. Images obtained from spatial opinion distributions (Section 3.2) were analyzed in terms of the grouping of opinions and the characteristics of these opinion clusters (Section 3.3). Based on the simulation results, we show how the number Φ^* of observed opinions (understood as spatial clusters of at least θ actors sharing the same opinion) depends on the model control parameters (effective range of interaction α and noise level T). In contrast to the Reference [56]— where the number of (arbitrarily recognized as small or large) cluster sizes were investigated—here we introduce the noise discrimination level θ allowing the finest analysis of histograms of cluster sizes.

As a square lattice is not best suited for modeling social interaction, also checking another network topology seems to be a promising way for further studies. On the other hand, the square lattice naturally produces a regular ego-centered network of actors [85–87], where nodes in subsequent coordination zones may be equated with subsequent 'circles' (in the ego-centered network theory terminology) containing the support clique (sites from the first and second coordination zones, Figure 2b), sympathy group (sites from the third to fifth coordination zones, the outermost 'ring' in Figure 2c), affinity group (sites from the sixth to the ninth coordination zones, the outermost 'ring' in Figure 2d) and active network (sites from the 10-th to 14-th coordination zones, not marked in Figure 2). Keeping the terminology of Reference [87], a 'red' actor presented in Figure 2a plays the role of 'ego' while actors in subsequent coordination zones are his/her 'alters'. Our results (Table 1) show that—independently of the number K of opinions available in the system—from 57% (low values of α in Equation (3)) to 99% (high values of α in Equation (3)) social impact on 'ego' comes from these five circles. We note that this effect is purely geometrical and should be recognized in any other topology of the underlying network of social contacts.

The maps shown in Figures 3, A3 indicate the tendency of the system to dominate only one opinion for $T > 1$ ultimately. With the available opinions, $K > 3$, by introducing a higher temperature T in the system, the share of dominant opinion in the entire system is reduced due to more spatially separated actors with different opinions. For the number of opinions $K = 5$ and the social temperature $T = 4$, this effect is magnified to such an extent that larger clusters in the system disappear, leading to an ever-changing random system state in which none of the available opinions prevail above the noise discrimination level θ.

High social temperature (observed, e.g., before elections) can be identified with high-mood liability, where many often consecutive events cause constant changes in individual opinions. A large part of voters do not know who to vote for; they have just started to think about it, their opinions are poorly established, and the final opinion is determined by random events.

As the exponent α increases in the distance scaling function, the system tends to form more and more clusters. On the other hand, increasing the social temperature T destroys the stability of the smaller clusters that exist in the system, which disappear in favor of the dominant clusters. However, as both values increase—especially for the large number of K opinions available in the system—agents' opinions become highly dispersed, and believers of the same opinion are unable to form large clusters. For high values of K, α, and T, the system is fragmented, and the state of the system is represented by dynamically changing and randomly distributed clusters on the grid, and each opinion has a similar number of agents believing in it.

Increasing the discrimination coefficient decreases the importance of small—spatially separated—groups of agents sharing a given opinion in the measurement of opinions. This may contribute to the impression of strong polarization in the system, giving a vision of the

presence of well-established divisions in society. This, in turn, may promote the image of a deep conflict between members of society, for example, between the voters of the two main political forces, creating the impression of a high electoral threshold. This effect is clearly visible in Figure 7, where the successive increase in θ leads to the systematic impression that the opinions of minorities (or at least their spatial dispersion) successively decrease the measured number Φ^* of the remaining opinions. This effect is best visible in the last row of Figure 7 (Figures 7j,l), that is, for a large number of available options ($K = 5$), where for the threshold $\theta = 50$ (Figure 7l) regardless of the influence of the effective interaction range α or the social temperature T, we do not observe a group of followers of the fifth opinion, and followers of the fourth opinion appear only marginally with only one of the examined sets of parameters ($\alpha = 3$ and $T = 0$). On the one hand, this can be a hint for manipulators of public opinion, and on the other hand, it can suggest how to oppose such manipulation effectively.

We emphasize that the concept of multiple opinions ($K \geq 3$) seems to be essential for the possibility of speaking about system polarization (which term is probably often overused in binary models of opinion formation). Based on the results collected in Table 1 we conclude that the larger α, the more influential the nearest neighbors are (see Section 3.1). The level of noise discrimination θ (allowing for detailed studies of the number Φ^* of surviving opinions) may be a useful tool for the analysis of social systems, not only in models of opinion dynamics.

The further direction of investigating this model may include checking the computational complexity, that is, the time to reach the equilibrium of the system as dependent on the size of the system or checking the influence of setting s_i and p_i in a way other than proposed here (i.e., taking them from normal instead of uniform distribution, or setting all of them to the same arbitrarily chosen values and reducing their space into only two parameters: $\forall i : s_i = s, p_i = p$).

Author Contributions: Conceptualization, K.M.; methodology, K.M.; software, M.D.; investigation, M.D. and K.M.; writing—original draft, K.M.; writing—review and editing, M.D. and K.M.; supervision, K.M. All authors have read and agreed to the published version of the manuscript.

Funding: This research received no external funding.

Data Availability Statement: The data generated by simulations is available from the authors upon a reasonable request. The source code is available online at [75].

Acknowledgments: We thank Krzysztof Kułakowski for a fruitful discussion and Jacek Tarasiuk for providing a nice random number generator. We thank anonymous Reviewers for pointing out the deficiency of the original manuscript, possible directions of further research and References [35,39] and particularly Reference [87] as well as for encouraging us to make the source code available online [75].

Conflicts of Interest: The authors declare no conflict of interest.

Appendix A. Examples of Final Spatial Opinion Distribution

Examples of the two most probable spatial distributions of the final opinion after $t = 10^3$ time steps of the system evolution for various noise levels T. The system contains $L^2 = 41^2$ actors. The exponent of the distance scaling function $\alpha = 3$ and the number of available opinions $K = 2$ (Figure A1), $\alpha = 3$ and $K = 2$ (Figure A2), $\alpha = 3$ and $K = 5$ (Figure A3), $\alpha = 4$ and $K = 2$ (Figure A4), $\alpha = 4$ and $K = 3$ (Figure A5), $\alpha = 4$ and $K = 4$ (Figure A6), $\alpha = 4$ and $K = 5$ (Figure A7).

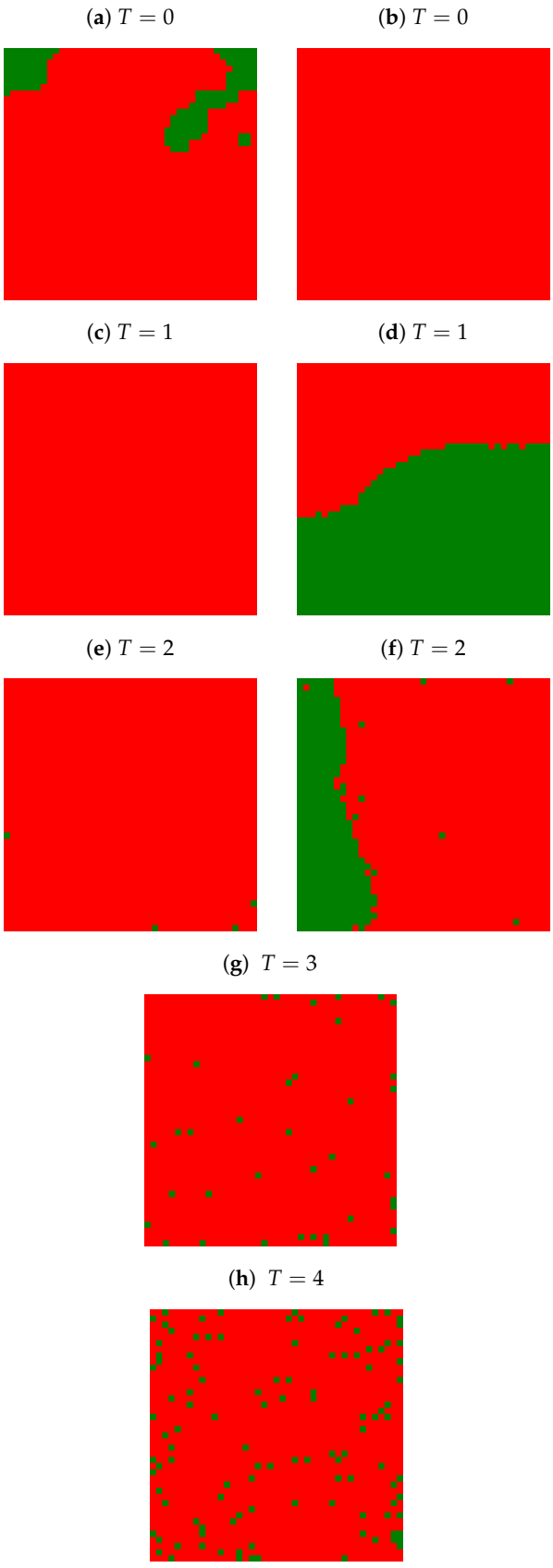

Figure A1. Examples of two most probable spatial distributions of the final opinion after 10^3 time steps. $L = 41$, $\alpha = 3$, $K = 2$ and various levels of noise T.

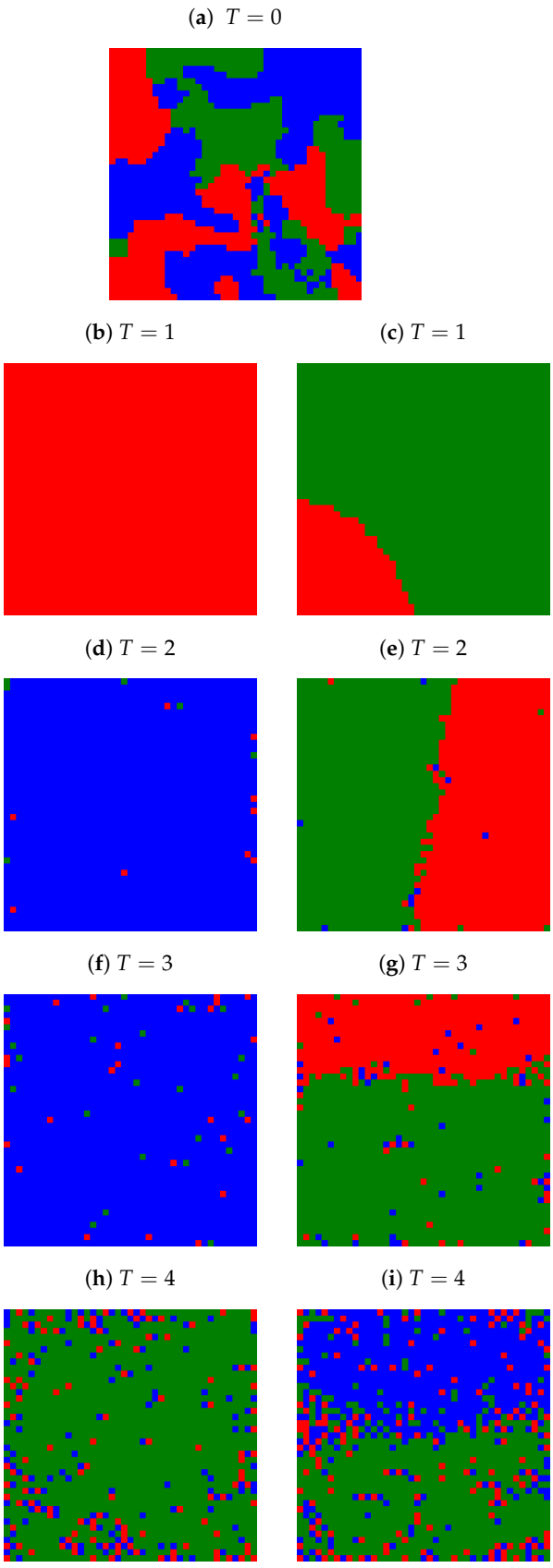

Figure A2. Examples of two most probable spatial distributions of the final opinion after 10^3 time steps. $L = 41$, $\alpha = 3$, $K = 3$ and various levels of noise T.

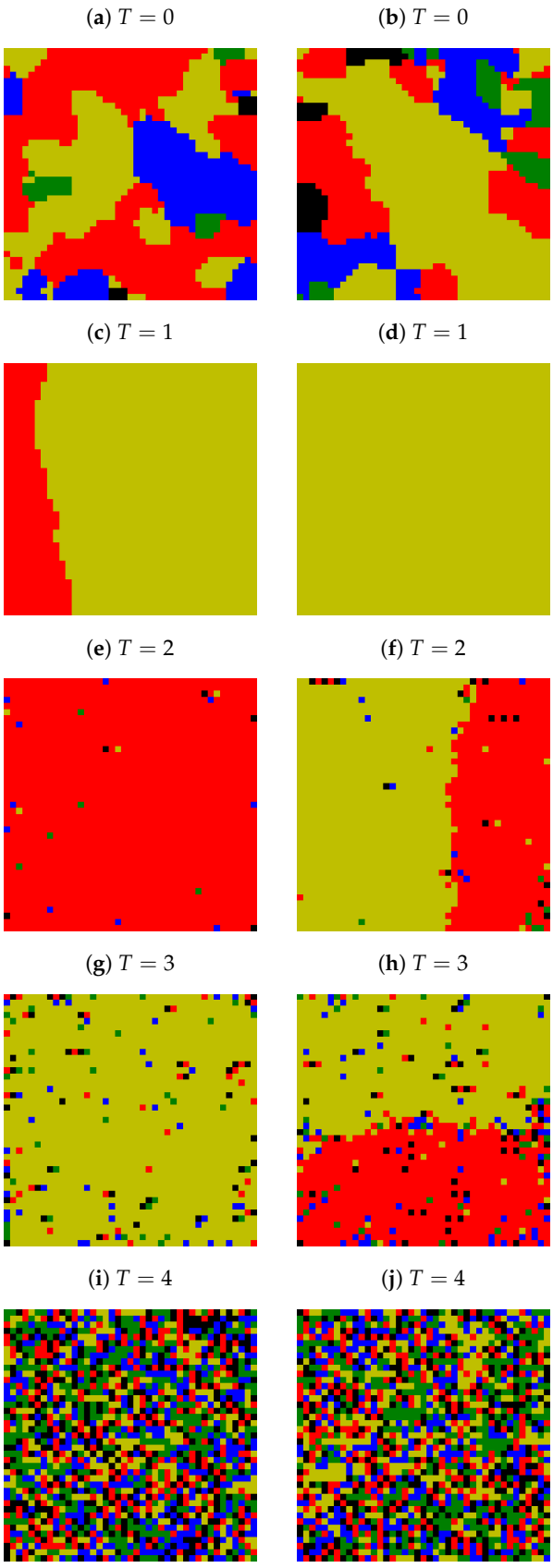

Figure A3. Examples of two most probable spatial distributions of the final opinion after 10^3 time steps. $L = 41$, $\alpha = 3$, $K = 5$ and various levels of noise T.

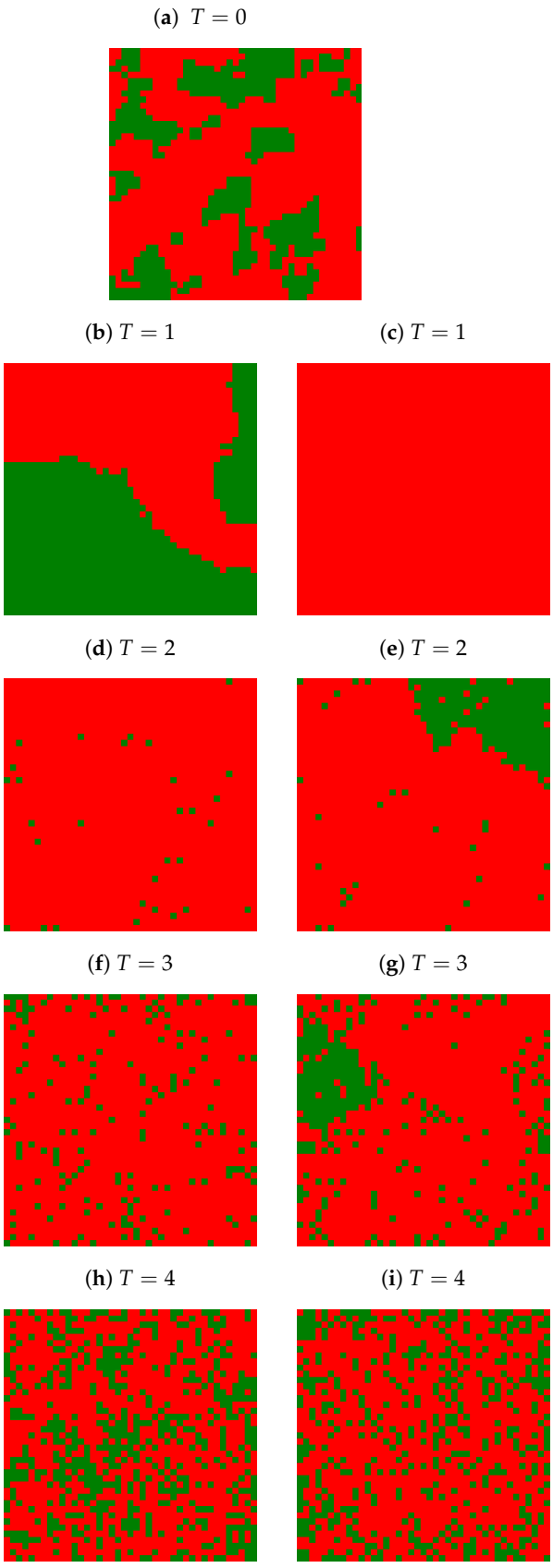

Figure A4. Examples of two most probable spatial distributions of the final opinion after 10^3 time steps. $L = 41$, $\alpha = 4$, $K = 2$ and various levels of noise T.

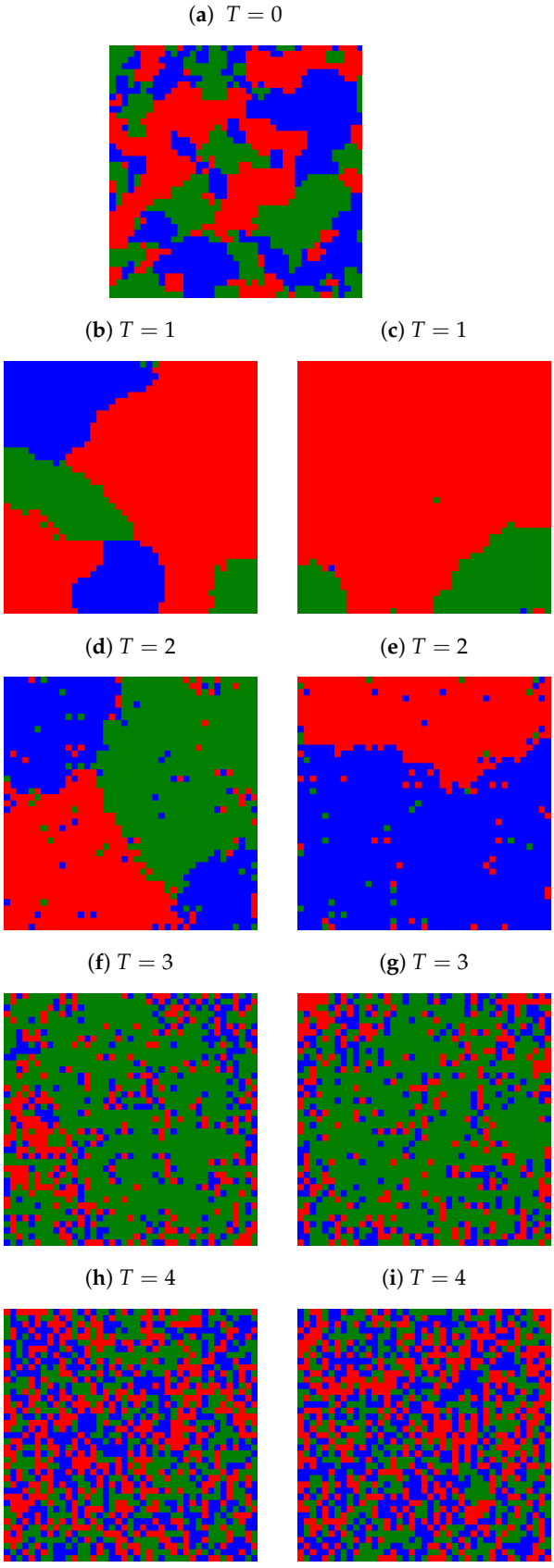

Figure A5. Examples of two most probable spatial distributions of the final opinion after 10^3 time steps. $L = 41$, $\alpha = 4$, $K = 3$ and various levels of noise T.

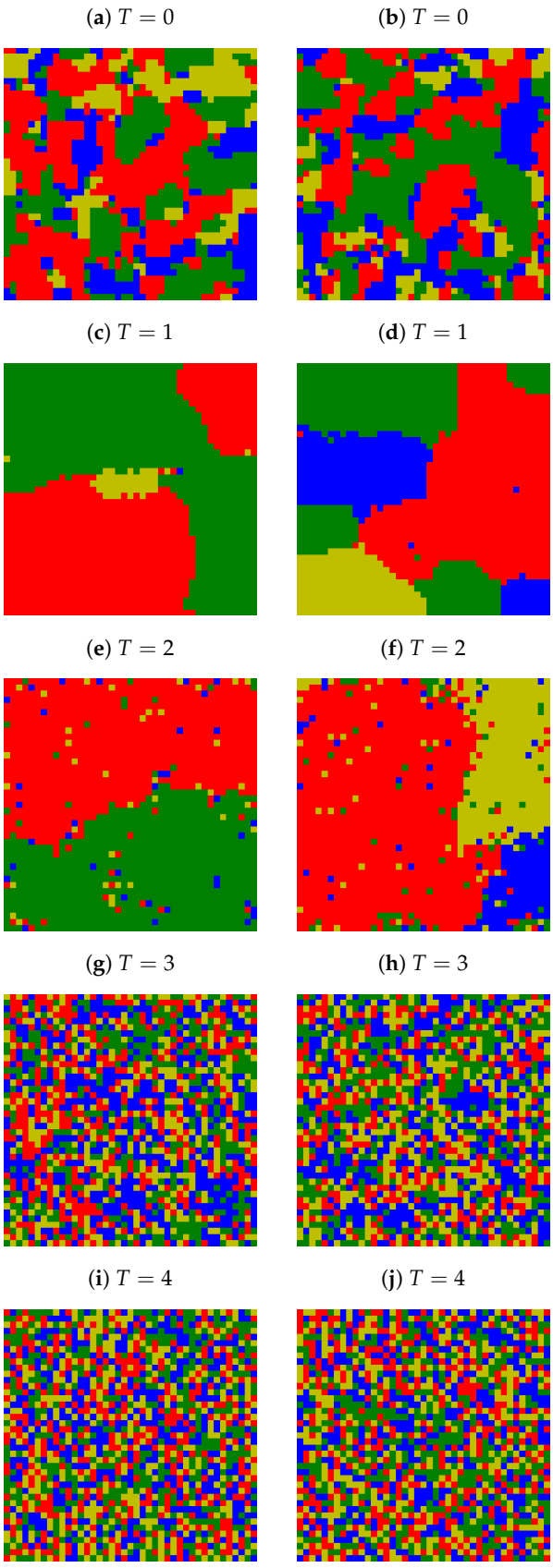

Figure A6. Examples of two most probable spatial distributions of the final opinion after 10^3 time steps. $L = 41$, $\alpha = 4$, $K = 4$ and various levels of noise T.

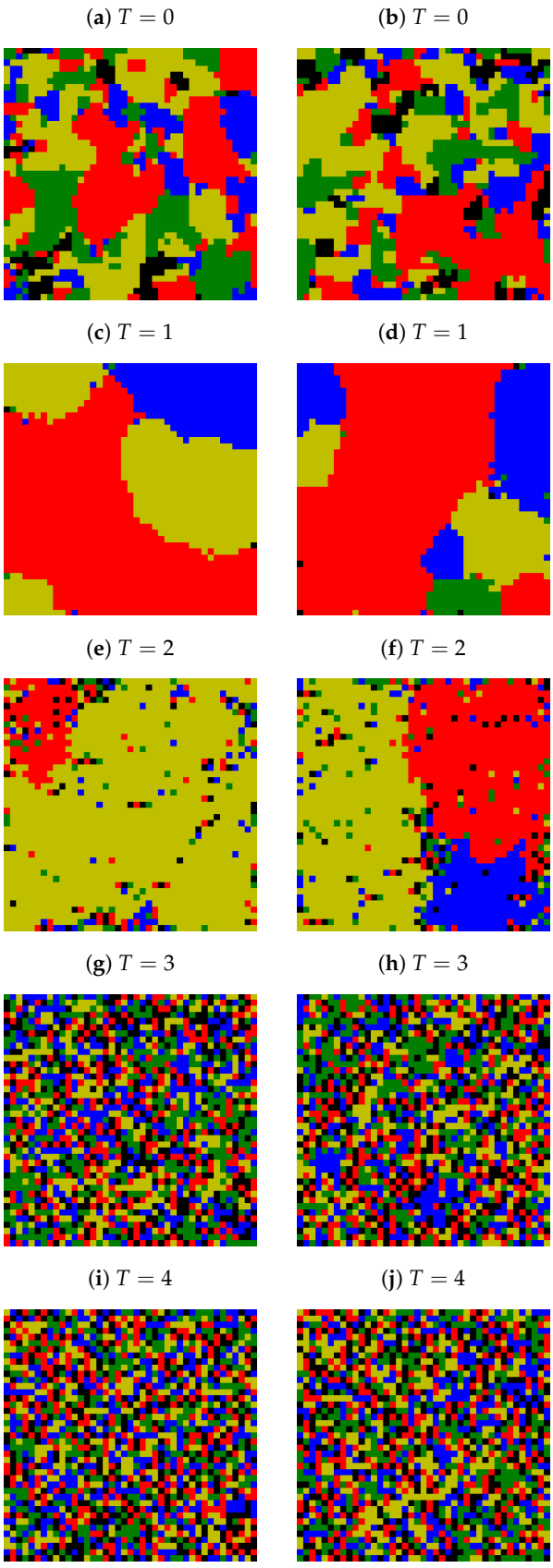

Figure A7. Examples of two most probable spatial distributions of the final opinion after 10^3 time steps. $L = 41$, $\alpha = 4$, $K = 5$ and various levels of noise T.

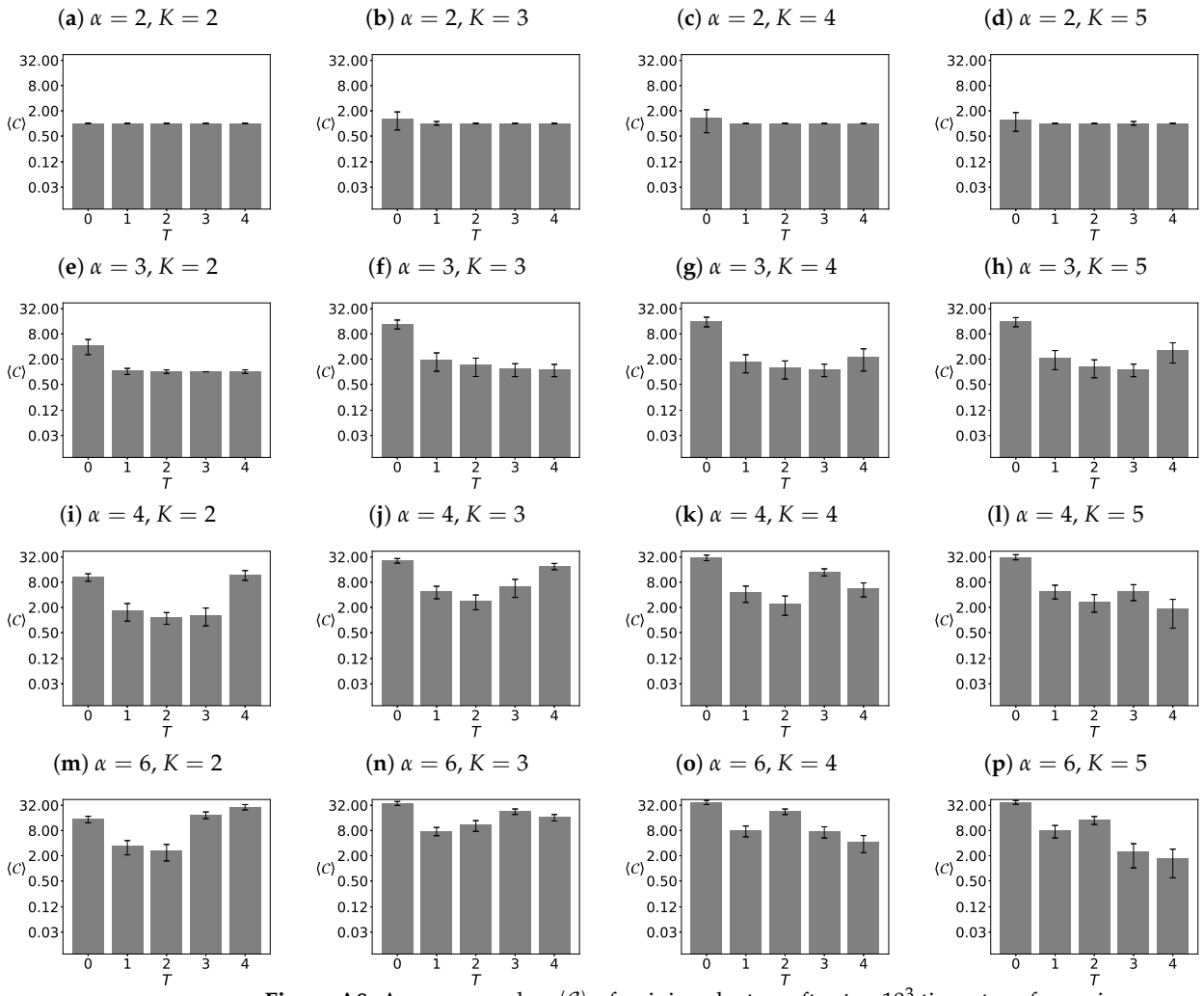

Figure A8. Average number $\langle \mathcal{C} \rangle$ of opinion clusters after $t = 10^3$ time steps for various exponents of the distance scaling function α and various numbers of available opinions K in the system. Noise discrimination threshold $\theta = 12$. The system contains $L^2 = 41^2$ actors. The results are averaged over $R = 100$ independent system realizations.

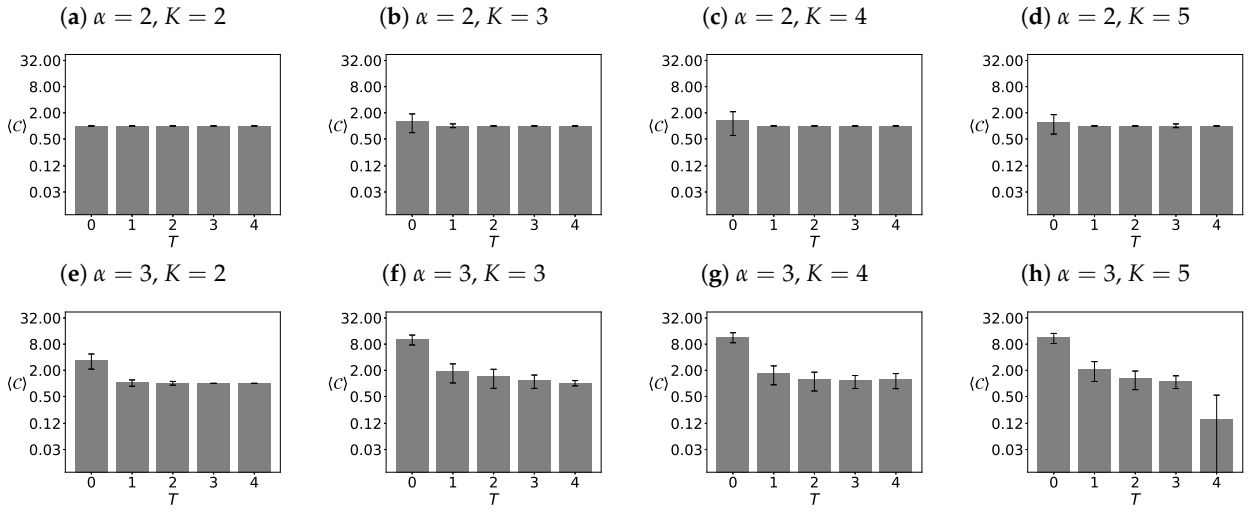

Figure A9. *Cont.*

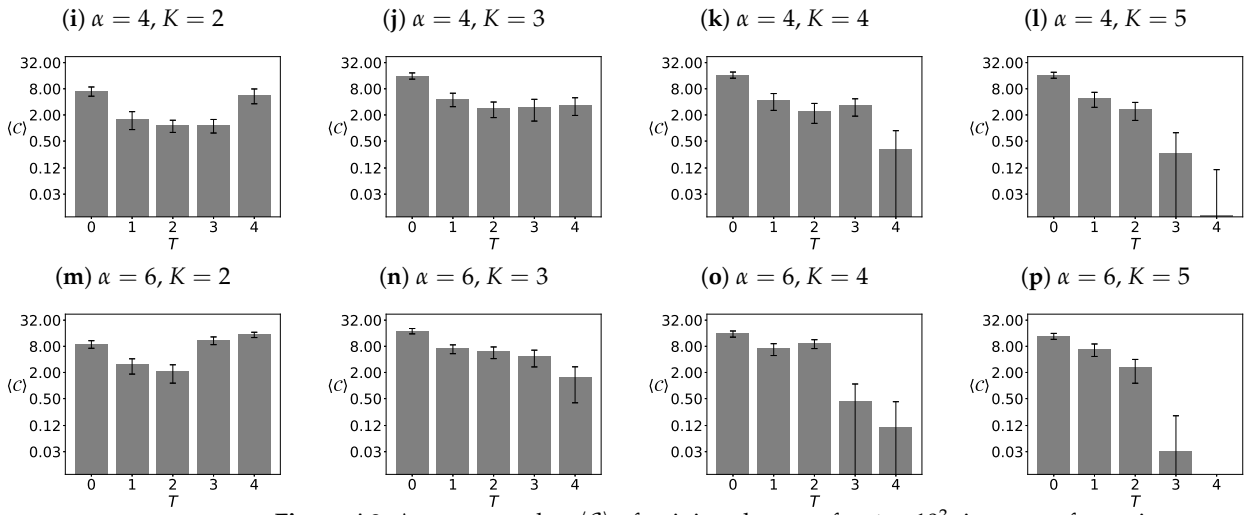

Figure A9. Average number $\langle \mathcal{C} \rangle$ of opinion clusters after $t = 10^3$ time steps for various exponents of the distance scaling function α and various numbers of available opinions K in the system. The noise discrimination threshold $\theta = 25$. The system contains $L^2 = 41^2$ actors. The results are averaged over $R = 100$ independent system realizations.

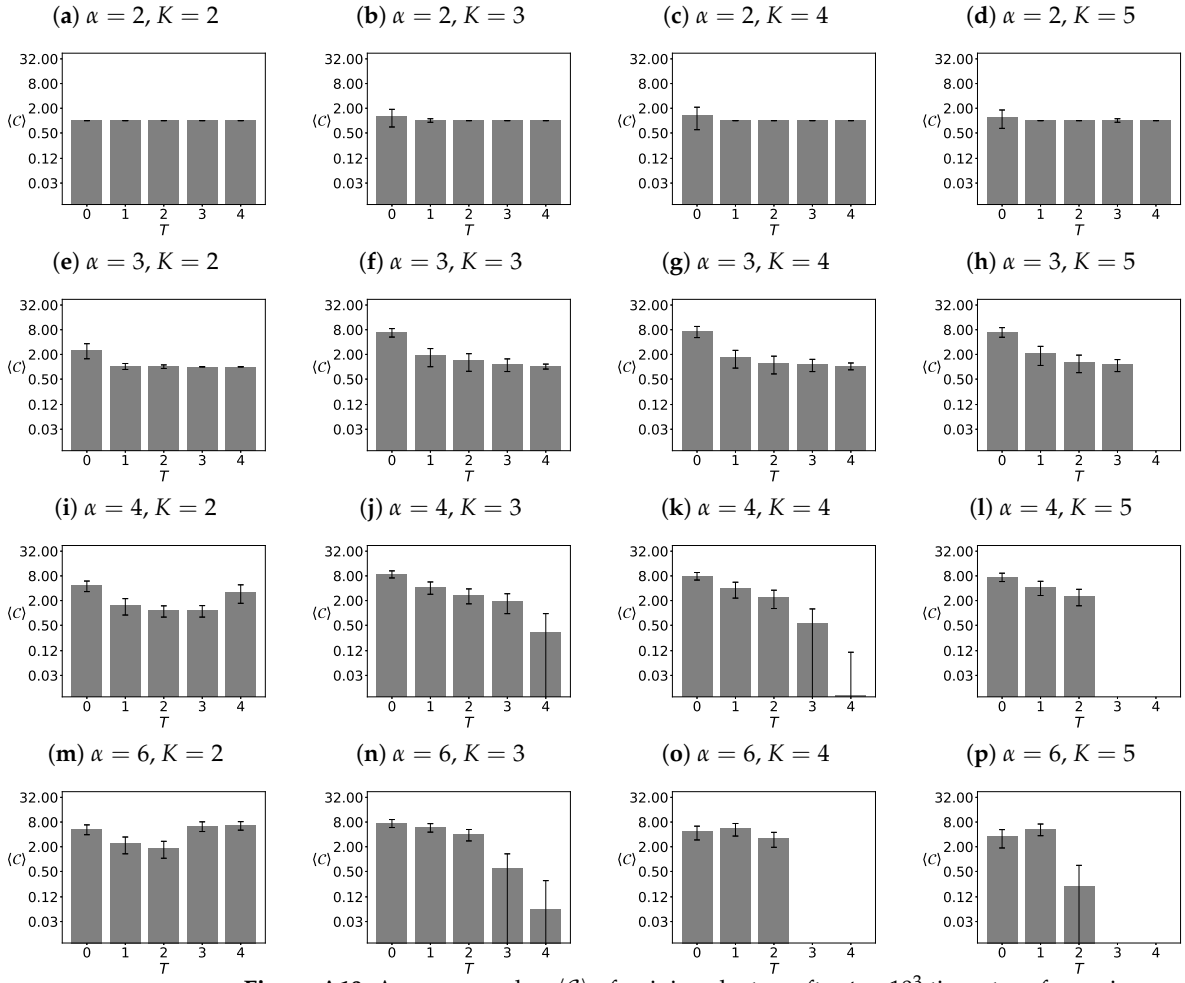

Figure A10. Average number $\langle \mathcal{C} \rangle$ of opinion clusters after $t = 10^3$ time steps for various exponents of the distance scaling function α and various numbers of available opinions K in the system. The noise discrimination threshold $\theta = 50$. The system contains $L^2 = 41^2$ actors. The results are averaged over $R = 100$ independent system realizations.

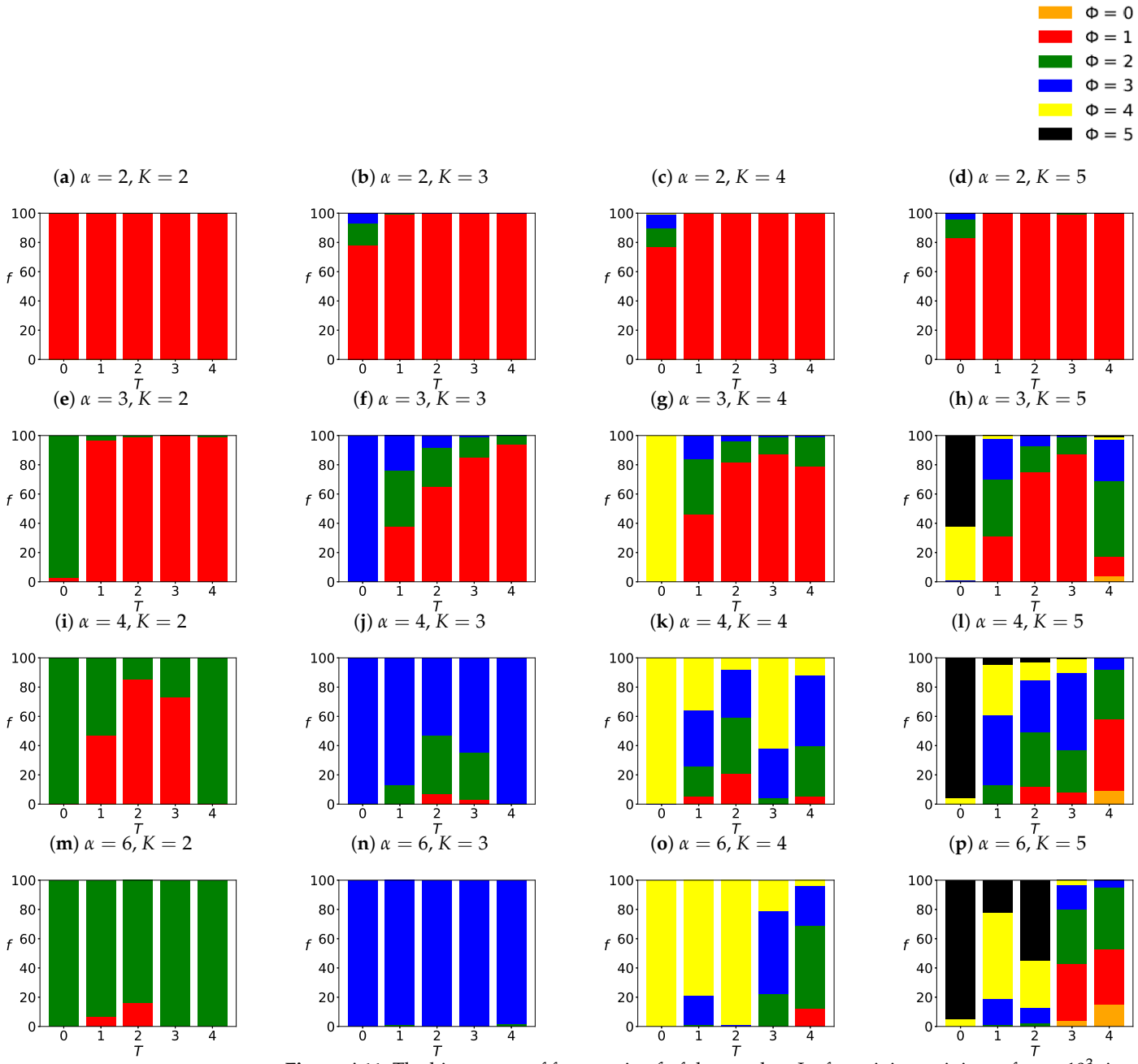

Figure A11. The histograms of frequencies f of the number Φ of surviving opinions after $= 10^3$ time steps and for various values of the distance scaling function exponent α and various values of the number of available opinions K. The system contains $L^2 = 41^2$ actors. The noise discrimination level $\theta = 12$ and the results are averaged over $R = 100$ independent simulations.

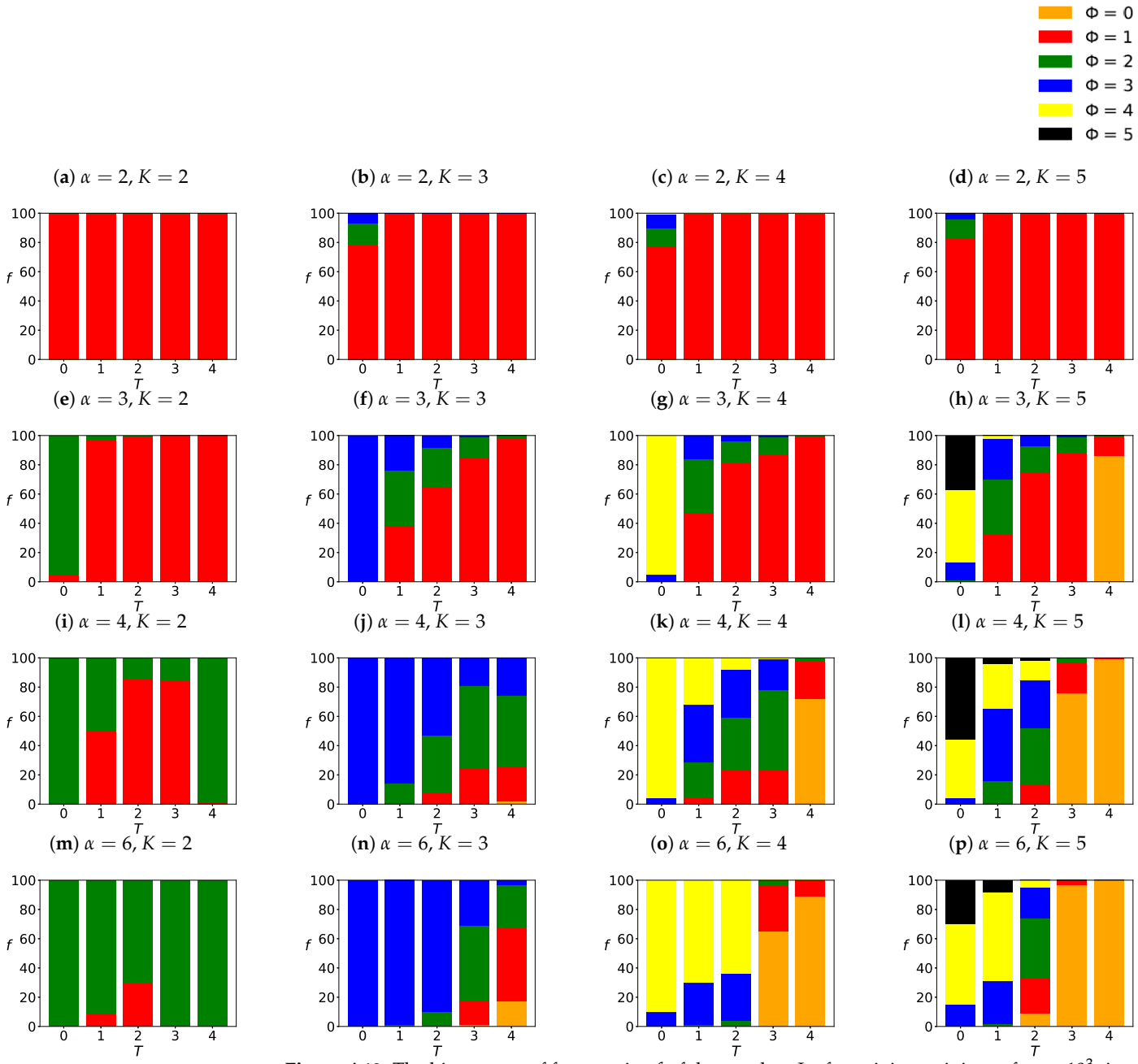

Figure A12. The histograms of frequencies f of the number Φ of surviving opinions after $= 10^3$ time steps and for various values of the distance scaling function exponent α and various values of the number of available opinions K. The system contains $L^2 = 41^2$ actors. The noise discrimination level $\theta = 25$ and the results are averaged over $R = 100$ independent simulations.

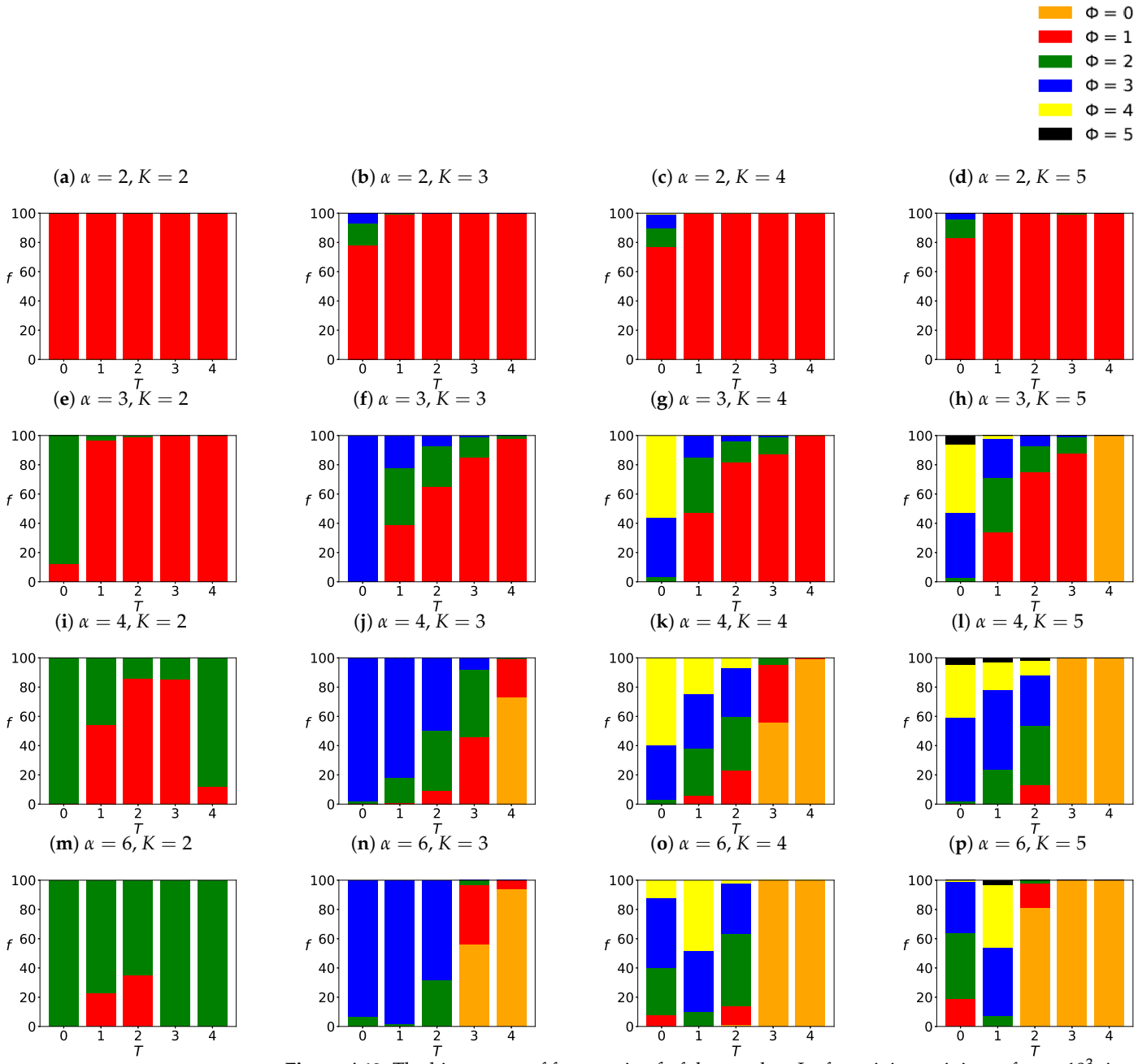

Figure A13. The histograms of frequencies f of the number Φ of surviving opinions after $= 10^3$ time steps and for various values of the distance scaling function exponent α and various values of the number of available opinions K. The system contains $L^2 = 41^2$ actors. The noise discrimination level $\theta = 50$ and the results are averaged over $R = 100$ independent simulations.

Appendix B. Average Number of Clusters

Average number $\langle \mathcal{C} \rangle$ of opinion clusters after $t = 10^3$ time steps for various exponents of the distance scaling function α and various numbers K of opinions available in the system. Noise discrimination threshold $\theta = 12$ (Figure A8), $\theta = 25$ (Figure A9), $\theta = 50$ (Figure A10). The system contains $L^2 = 41^2$ actors. The results are averaged over $R = 100$ independent system realisations.

Appendix C. The Number of Surviving Opinions

Histograms of the frequencies f of the number Φ of surviving opinions after $= 10^3$ time steps and for various values of the distance scaling function exponent α and various

values of the number of available opinions K. The system contains $L^2 = 41^2$ actors. The noise discrimination level $\theta = 12$ (Figure A11), $\theta = 25$ (Figure A12), $\theta = 50$ (Figure A13) and the results are averaged over $R = 100$ independent simulations.

References

1. Galam, S. Opinion Dynamics and Unifying Principles: A Global Unifying Frame. *Entropy* **2022**, *24*, 1201. [CrossRef]
2. Kozitsin, I. A general framework to link theory and empirics in opinion formation models. *Sci. Rep.* **2022**, *12*, 5543. [CrossRef]
3. Weron, T.; Szwabiński, J. Opinion Evolution in Divided Community. *Entropy* **2022**, *24*, 185. [CrossRef]
4. Galam, S.; Brooks, R.R.W. Radicalism: The asymmetric stances of radicals versus conventionals. *Phys. Rev. E* **2022**, *105*, 044112. [CrossRef]
5. Muslim, R.; Kholili, M.; Nugraha, A. Opinion dynamics involving contrarian and independence behaviors based on the Sznajd model with two-two and three-one agent interactions. *Phys. D Nonlinear Phenom.* **2022**, *439*, 133379. [CrossRef]
6. Lian, Y.; Dong, X. An opinion dynamics model for unrelated discrete opinions. *Knowl.-Based Syst.* **2022**, *251*, 109133. [CrossRef]
7. Su, W.; Chen, X.; Yu, Y.; Chen, G. Noise-Based Control of Opinion Dynamics. *IEEE Trans. Autom. Control* **2022**, *67*, 3134–3140. [CrossRef]
8. Zachary, D.S. Modelling shifts in social opinion through an application of classical physics. *Sci. Rep.* **2022**, *12*, 5485. [CrossRef]
9. Nguyen, V.X.; Xiao, G.; Xu, X.J.; Wu, Q.; Xia, C.Y. Dynamics of opinion formation under majority rules on complex social networks. *Sci. Rep.* **2020**, *10*, 456. [CrossRef]
10. Galam, S.; Cheon, T. Asymmetric Contrarians in Opinion Dynamics. *Entropy* **2020**, *22*, 25. [CrossRef]
11. Galam, S.; Cheon, T. Tipping Points in Opinion Dynamics: A Universal Formula in Five Dimensions. *Front. Phys.* **2020**, *8*, 566580. [CrossRef]
12. Malarz, K.; Szvetelszky, Z.; Szekfü, B.; Kułakowski, K. Gossip in random networks. *Acta Phys. Pol. B* **2006**, *37*, 3049–3058.
13. Choi, D.; Chun, S.; Oh, H.; Han, J.; Kwon, T.T. Rumor Propagation is Amplified by Echo Chambers in Social Media. *Sci. Rep.* **2020**, *10*, 310. [CrossRef]
14. Castellano, C.; Fortunato, S.; Loreto, V. Statistical physics of social dynamics. *Rev. Mod. Phys.* **2009**, *81*, 591–646. [CrossRef]
15. Stauffer, D. A Biased Review of Sociophysics. *J. Stat. Phys.* **2013**, *151*, 9–20. [CrossRef]
16. Galam, S. The Trump phenomenon: An explanation from sociophysics. *Int. J. Mod. Phys. B* **2017**, *31*, 1742015. [CrossRef]
17. Ishii, A.; Kawahata, Y. Sociophysics analysis of the dynamics of peoples' interests in society. *Front. Phys.* **2018**, *6*, 089. [CrossRef]
18. Schweitzer, F. Sociophysics. *Phys. Today* **2018**, *71*, 40–46. [CrossRef]
19. Sobkowicz, P. Social Simulation Models at the Ethical Crossroads. *Sci. Eng. Ethics* **2019**, *25*, 143–157. [CrossRef]
20. Jusup, M.; Holme, P.; Kanazawa, K.; Takayasu, M.; Romić, I.; Wang, Z.; Geček, S.; Lipić, T.; Podobnik, B.; Wang, L.; et al. Social physics. *Phys. Rep.* **2022**, *948*, 1–148. [CrossRef]
21. Fortunato, S.; Stauffer, D. Computer Simulations of Opinions. *arXiv* **2005**. [CrossRef]
22. Grabisch, M.; Rusinowska, A. A Survey on Nonstrategic Models of Opinion Dynamics. *Games* **2020**, *11*, 65. [CrossRef]
23. Hegselmann, R.; Krause, U. Opinion dynamics and bounded confidence: Models, analysis and simulation. *JASSS— J. Artif. Soc. Soc. Simul.* **2002**, *5*, 2.
24. Schawe, H.; Hernández, L. When open mindedness hinders consensus. *Sci. Rep.* **2020**, *10*, 8273. [CrossRef]
25. Schawe, H.; Hernández, L. Collective effects of the cost of opinion change. *Sci. Rep.* **2020**, *10*, 13825. [CrossRef]
26. Deffuant, G.; Neau, D.; Amblard, F.; Weisbuch, G. Mixing beliefs among interacting agents. *Adv. Complex Syst.* **2000**, *3*, 87. [CrossRef]
27. Deffuant, G. Comparing extremism propagation patterns in continuous opinion models. *JASSS— J. Artif. Soc. Soc. Simul.* **2006**, *9*, 8.
28. Malarz, K. Truth seekers in opinion dynamics models. *Int. J. Mod. Phys. C* **2006**, *17*, 1521–1524. [CrossRef]
29. Mathias, J.D.; Huet, S.; Deffuant, G. Bounded confidence model with fixed uncertainties and extremists: The opinions can keep fluctuating indefinitely. *JASSS— J. Artif. Soc. Soc. Simul.* **2016**, *19*, 6. [CrossRef]
30. Chen, G.; Cheng, H.; Huang, C.; Han, W.; Dai, Q.; Li, H.; Yang, J. Deffuant model on a ring with repelling mechanism and circular opinions. *Phys. Rev. E* **2017**, *95*, 042118. [CrossRef]
31. Kułakowski, K. Opinion polarization in the Receipt–Accept–Sample model. *Physica A* **2009**, *388*, 469–476. [CrossRef]
32. Malarz, K.; Gronek, P.; Kułakowski, K. Zaller–Deffuant model of mass opinion. *JASSS— J. Artif. Soc. Soc. Simul.* **2011**, *14*, 2. [CrossRef]
33. Malarz, K.; Kułakowski, K. Bounded confidence model: Addressed information maintain diversity of opinions. *Acta Phys. Pol. A* **2012**, *121*, B86–B88. [CrossRef]
34. Malarz, K.; Kułakowski, K. Mental ability and common sense in an artificial society. *Europhys. News* **2014**, *45*, 21–23. [CrossRef]
35. Weisbuch, G.; Deffuant, G.; Amblard, F.; Nadal, J.P. Interacting Agents and Continuous Opinions Dynamics. In *Heterogenous Agents, Interactions and Economic Performance*; Cowan, R., Jonard, N., Eds.; Springer: Berlin/Heidelberg, Germany, 2003; pp. 225–242. [CrossRef]
36. Ben-Naim, E.; Krapivsky, P.L.; Redner, S. Bifurcations and patterns in compromise processes. *Phys. D Nonlinear Phenom.* **2003**, *183*, 190–204. [CrossRef]

37. Ben-Naim, E.; Krapivsky, P.L.; Vazquez, F.; Redner, S. Unity and discord in opinion dynamics. *Phys. A Stat. Mech. Its Appl.* **2003**, *330*, 99–106. [CrossRef]
38. Weisbuch, G.; Deffuant, G.; Amblard, F.; Nadal, J.P. Meet, discuss, and segregate! *Complexity* **2002**, *7*, 55–63. [CrossRef]
39. Laguna, M.F.; Abramson, G.; Zanette, D.H. Minorities in a model for opinion formation. *Complexity* **2004**, *9*, 31–36. [CrossRef]
40. Galam, S. Minority opinion spreading in random geometry. *Eur. Phys. J. B* **2002**, *25*, 403–406. [CrossRef]
41. Oliveira, L.S.; Rodrigues, A.C.; Forgerini, F.L. Reputation in Majority Rule Model leading to democratic states. *J. Phys. Conf. Ser.* **2019**, *1391*, 012042. [CrossRef]
42. Holley, R.A.; Liggett, T.M. Ergodic theorems for weakly interacting infinite systems and voter model. *Ann. Probab.* **1975**, *3*, 643–663. [CrossRef]
43. Lima, F.W.S.; Malarz, K. Majority-vote model on $(3,4,6,4)$ and $(3^4,6)$ Archimedean lattices. *Int. J. Mod. Phys. C* **2006**, *17*, 1273–1283. [CrossRef]
44. Fernandez-Gracia, J.; Suchecki, K.; Ramasco, J.J.; San Miguel, M.; Eguiluz, V.M. Is the Voter Model a Model for Voters? *Phys. Rev. Lett.* **2014**, *112*, 158701. [CrossRef] [PubMed]
45. Sznajd-Weron, K.; Sznajd, J. Opinion evolution in closed community. *Int. J. Mod. Phys. C* **2000**, *11*, 1157–1165. [CrossRef]
46. Sznajd-Weron, K. Sznajd model and its applications. *Acta Phys. Pol. B* **2005**, *36*, 2537–2547.
47. Sznajd-Weron, K.; Sznajd, J. Who is left, who is right? *Physica A* **2005**, *351*, 593–604. [CrossRef]
48. Malarz, K.; Kułakowski, K. The Sznajd dynamics on a directed clustered network. *Acta Phys. Pol. A* **2008**, *114*, 581–588. [CrossRef]
49. Sznajd-Weron, K.; Sznajd, J.; Weron, T. A review on the Sznajd model—20 years after. *Physica A* **2021**, *565*, 125537. [CrossRef]
50. Galam, S. Unifying Local Dynamics in Two-State Spin Systems. *arXiv* **2004**. [CrossRef]
51. Galam, S. Sociophysics: A review of Galam models. *Int. J. Mod. Phys. C* **2008**, *19*, 409–440. [CrossRef]
52. Gekle, S.; Peliti, L.; Galam, S. Opinion dynamics in a three-choice system. *Eur. Phys. J. B* **2005**, *45*, 569–575. [CrossRef]
53. Malarz, K.; Kułakowski, K. Indifferents as an interface between Contra and Pro. *Acta Phys. Pol. A* **2010**, *117*, 695–699. [CrossRef]
54. Öztürk, M.K. Dynamics of discrete opinions without compromise. *Adv. Complex Syst.* **2013**, *16*, 1350010. [CrossRef]
55. Bańcerowski, P.; Malarz, K. Multi-choice opinion dynamics model based on Latané theory. *Eur. Phys. J. B* **2019**, *92*, 219. [CrossRef]
56. Kowalska-Styczeń, A.; Malarz, K. Noise induced unanimity and disorder in opinion formation. *PLoS ONE* **2020**, *15*, e0235313. [CrossRef]
57. Martins, A.C.R. Discrete opinion dynamics with M choices. *Eur. Phys. J. B* **2020**, *93*, 1. [CrossRef]
58. Zubillaga, B.; Vilela, A.; Wang, M.; Du, R.; Dong, G.; Stanley, H. Three-state majority-vote model on small-world networks. *Sci. Rep.* **2022**, *12*, 282. [CrossRef]
59. Li, L.; Zeng, A.; Fan, Y.; Di, Z. Modeling multi-opinion propagation in complex systems with heterogeneous relationships via Potts model on signed networks. *Chaos* **2022**, *32*, 083101. [CrossRef]
60. Doniec, M.; Lipiecki, A.; Sznajd-Weron, K. Consensus, Polarization and Hysteresis in the Three-State Noisy q-Voter Model with Bounded Confidence. *Entropy* **2022**, *24*, 983. [CrossRef]
61. Xiong, F.; Liu, Y.; Wang, L.; Wang, X. Analysis and application of opinion model with multiple topic interactions. *Chaos* **2017**, *27*, 083113. [CrossRef]
62. Galam, S. The drastic outcomes from voting alliances in three-party democratic voting (1990–2013). *J. Stat. Phys.* **2013**, *151*, 46–68. [CrossRef]
63. Wu, D.; Szeto, K.Y. Analysis of timescale to consensus in voting dynamics with more than two options. *Phys. Rev. E* **2018**, *97*, 042320. [CrossRef] [PubMed]
64. Nowak, A.; Szamrej, J.; Latané, B. From private attitude to public opinion: A dynamic theory of social impact. *Psychol. Rev.* **1990**, *97*, 362–376. [CrossRef]
65. Darley, J.M.; Latané, B. Bystander intervention in emergencies—Diffusion of responsibility. *J. Personal. Soc. Psychol.* **1968**, *8*, 377–383. [CrossRef] [PubMed]
66. Latané, B.; Harkins, S. Cross-modality matches suggest anticipated stage fright a multiplicative power function of audience size and status. *Percept. Psychophys.* **1976**, *20*, 482–488. [CrossRef]
67. Latané, B. The psychology of social impact. *Am. Psychol.* **1981**, *36*, 343–356. [CrossRef]
68. Kacperski, K.; Hołyst, J.A. Phase transitions as a persistent feature of groups with leaders in models of opinion formation. *Physica A* **2000**, *287*, 631–643. [CrossRef]
69. Hołyst, J.A.; Kacperski, K.; Schweitzer, F. Phase transitions in social impact models of opinion formation. *Physica A* **2000**, *285*, 199–210. [CrossRef]
70. Kowalska-Styczeń, A.; Malarz, K. Are randomness of behavior and information flow important to opinion forming in organization? In Proceedings of the 36th International Business Information Management Association Conference, Granada, Spain, 4–5 November 2020; Soliman, K.S., Ed.; International Business Information Management Associationa: King of Prussia, PA, USA, 2020; pp. 10691–10698. [CrossRef]
71. Hołyst, J.A.; Kacperski, K.; Schweitzer, F. Social Impact Models of Opinion Dynamics. In *Annual Reviews of Computational Physics IX*; Stauffer, D., Ed.; World Scientific: Singapore, 2011; pp. 253–273. [CrossRef]
72. Bańcerowski, P. Modeling of Opinion Formation Based on Latané Theory. Master's Thesis, AGH University of Science and Technology, Kraków, Poland, 2017. (In Polish)

73. Dworak, M. Modeling of Public Opinion Dynamics in a System with Many Available Discrete Opinions. Master's Thesis, AGH University of Science and Technology, Kraków, Poland, 2022. (In Polish)
74. Kułakowski, K. A note on temperature without energy—A social example. *arXiv* **2008**, arXiv:0807.0711.
75. Available online: http://www.zis.agh.edu.pl/app/MSc/Maciej_Dworak/ (accessed on 5 December 2022).
76. Landau, D.P.; Binder, K. *A Guide to Monte Carlo Simulations in Statistical Physics*, 3rd ed.; Cambridge University Press: Cambridge, UK, 2009. [CrossRef]
77. Hoshen, J.; Kopelman, R. Percolation and cluster distribution. 1. Cluster multiple labeling technique and critical concentration algorithm. *Phys. Rev. B* **1976**, *14*, 3438–3445. [CrossRef]
78. Frijters, S.; Krüger, T.; Harting, J. Parallelised Hoshen–Kopelman algorithm for lattice-Boltzmann simulations. *Comput. Phys. Commun.* **2015**, *189*, 92–98. [CrossRef]
79. Kotwica, M.; Gronek, P.; Malarz, K. Efficient space virtualisation for Hoshen–Kopelman algorithm. *Int. J. Mod. Phys. C* **2019**, *30*, 1950055. [CrossRef]
80. Ren, J.; Wang, W.X.; Qi, F. Randomness enhances cooperation: A resonance-type phenomenon in evolutionary games. *Phys. Rev. E* **2007**, *75*, 045101. [CrossRef] [PubMed]
81. Shirado, H.; Christakis, N.A. Locally noisy autonomous agents improve global human coordination in network experiments. *Nature* **2017**, *545*, 370–374. [CrossRef] [PubMed]
82. De Sanctis, L.; Galla, T. Effects of noise and confidence thresholds in nominal and metric Axelrod dynamics of social influence. *Phys. Rev. E* **2009**, *79*, 046108. [CrossRef] [PubMed]
83. Biondo, A.E.; Pluchino, A.; Rapisarda, A. The Beneficial Role of Random Strategies in Social and Financial Systems. *J. Stat. Phys.* **2013**, *151*, 607–622. [CrossRef]
84. Su, W.; Chen, G.; Hong, Y. Noise leads to quasi-consensus of Hegselmann–Krause opinion dynamics. *Automatica* **2017**, *85*, 448–454. [CrossRef]
85. Dunbar, R.; Gamble, C.; Gowlett, J. *Social Brain, Distributed Mind*; British Academy: London, UK, 2010. [CrossRef]
86. Sutcliffe, A.; Dunbar, R.; Binder, J.; Arrow, H. Relationships and the social brain: Integrating psychological and evolutionary perspectives. *Br. J. Psychol.* **2012**, *103*, 149–168. [CrossRef]
87. Arnaboldi, V.; Conti, M.; La Gala, M.; Passarella, A.; Pezzoni, F. Ego network structure in online social networks and its impact on information diffusion. *Comput. Commun.* **2016**, *76*, 26–41. [CrossRef]

Disclaimer/Publisher's Note: The statements, opinions and data contained in all publications are solely those of the individual author(s) and contributor(s) and not of MDPI and/or the editor(s). MDPI and/or the editor(s) disclaim responsibility for any injury to people or property resulting from any ideas, methods, instructions or products referred to in the content.